



HAL
open science

Contribution of close-in fallout from the French atmospheric tests in inventories of ^{137}Cs , ^{241}Am and plutonium (238 , 239 , 240) in Gambier Islands (French Polynesia) – Signatures of stratospheric fallout in the Southern Hemisphere

P. Bouisset, M Nohl, Catherine Cossonnet, Beatrice Boulet, Sandrine Thomas, Nicolas Cariou, Gilles Salaun

► To cite this version:

P. Bouisset, M Nohl, Catherine Cossonnet, Beatrice Boulet, Sandrine Thomas, et al.. Contribution of close-in fallout from the French atmospheric tests in inventories of ^{137}Cs , ^{241}Am and plutonium (238 , 239 , 240) in Gambier Islands (French Polynesia) – Signatures of stratospheric fallout in the Southern Hemisphere. *Journal of Environmental Radioactivity*, 2021, 235-236, pp.106624. 10.1016/j.jenvrad.2021.106624 . hal-03360613

HAL Id: hal-03360613

<https://hal.science/hal-03360613>

Submitted on 1 Oct 2021

HAL is a multi-disciplinary open access archive for the deposit and dissemination of scientific research documents, whether they are published or not. The documents may come from teaching and research institutions in France or abroad, or from public or private research centers.

L'archive ouverte pluridisciplinaire **HAL**, est destinée au dépôt et à la diffusion de documents scientifiques de niveau recherche, publiés ou non, émanant des établissements d'enseignement et de recherche français ou étrangers, des laboratoires publics ou privés.



Distributed under a Creative Commons Attribution - NonCommercial - NoDerivatives 4.0 International License

Contribution of local fallout from the French atmospheric tests in inventories of ^{137}Cs , ^{241}Am and plutonium (238, 239, 240) in Gambier Islands (French Polynesia) - Signatures of stratospheric fallout in the Southern Hemisphere.

ABSTRACT

The inventories of ^{137}Cs ($499 \pm 34 \text{ Bq.m}^{-2}$), ^{241}Am ($11.3 \pm 1.2 \text{ Bq.m}^{-2}$), ^{241}Pu ($33.7 \pm 3.4 \text{ Bq.m}^{-2}$), ^{238}Pu ($6.82 \pm 0.87 \text{ Bq.m}^{-2}$) and $^{239+240}\text{Pu}$ ($113.0 \pm 5.9 \text{ Bq.m}^{-2}$), sum of ^{239}Pu ($106 \pm 11 \text{ Bq.m}^{-2}$) and ^{240}Pu ($14.7 \pm 1.7 \text{ Bq.m}^{-2}$), in the Gambier archipelago (24°S) of the French Polynesia, are well higher than the global fallout at this latitude, in unequal proportions for the different radionuclides. $(^{240}\text{Pu}/^{239}\text{Pu})_{\text{AR}}$ of 0.0401 ± 0.0043 , and $(^{241}\text{Pu}/^{239}\text{Pu})_{\text{AR}}$ of $(2.04 \pm 0.32)10^{-4}$, confirm that the overwhelmingly dominant source of these radionuclides comes from local fallout during the 1970s of the French atmospheric tests of Moruroa and Fangataufa located nearly 400 km from the Gambier. The signatures of the local fallout were deduced from the excess of its inventory in ^{137}Cs and from the mixing lines established from the signatures of the global fallout, some of the test sites and the isotopic ratios measured in the Gambier. Signatures obtained are 2.0 ± 0.4 for $^{137}\text{Cs}/^{239+240}\text{Pu}$, 0.045 ± 0.008 for $^{238}\text{Pu}/^{239+240}\text{Pu}$, 0.031 ± 0.009 for $^{241}\text{Am}/^{239+240}\text{Pu}$, 0.092 ± 0.027 for $^{241}\text{Pu}/^{239+240}\text{Pu}$, 0.0176 ± 0.0049 for $(^{240}\text{Pu}/^{239}\text{Pu})_{\text{AR}}$, $(0.55 \pm 0.23)10^{-4}$ for $(^{241}\text{Pu}/^{239}\text{Pu})_{\text{AR}}$. The concordance of the mixing lines of the $[(^{240}\text{Pu}/^{239}\text{Pu})_{\text{AR}}, (^{241}\text{Pu}/^{239}\text{Pu})_{\text{AR}}]$ and the linear regression of these ratios measured in the stratosphere (40°S) during the 1970s, indicates that the signatures of the local fallout are also those of the stratospheric injections of the French tests. The signatures of stratospheric fallout in the Southern Hemisphere were evaluated by considering that the fission energy of these injections represents 11% and that of the Northern Hemisphere represents 89%. The activity ratios deduced are 21.9 ± 0.1 in $^{137}\text{Cs}/^{239+240}\text{Pu}$, 0.11 ± 0.05 in $^{238}\text{Pu}/^{239+240}\text{Pu}$, 1.03 ± 0.12 in $^{241}\text{Pu}/^{239+240}\text{Pu}$ and 0.35 ± 0.05 in $^{241}\text{Am}/^{239+240}\text{Pu}$. The associated atom ratios are 0.157 ± 0.011 for $(^{240}\text{Pu}/^{239}\text{Pu})_{\text{AR}}$ and $(8.28 \pm 0.18)10^{-4}$ for $(^{241}\text{Pu}/^{239}\text{Pu})_{\text{AR}}$. These signatures appear to be consistent with the results of the inventories at Hiva Oa, located more than 1,000 km north of both French test sites, and with those found in the Australian continent, in regions not impacted by UK-test debris. The proportions of close-in tropospheric fallout from the French tests are about 90% in the Gambier. They represent a proportion in the inventories of 40% for the ^{137}Cs , ^{241}Pu and ^{241}Am , 75% for ^{238}Pu and 90% for $^{239+240}\text{Pu}$.

Keywords: Inventory, Close-in deposition, Stratospheric signatures, Pu atom ratios, ^{137}Cs , ^{241}Am , Gambier, French atmospheric tests

Auteurs :

P. Bouisset(a), M. Nohl(a), C. Cossonnet(b), B. Boulet(b), S. Thomas(b), N. Cariou(b), G. Salaun(c)

a Institut de Radioprotection et de Sûreté nucléaire, BP 182, 98725, Vairao, Tahiti, French Polynesia

b Institut de Radioprotection et de Sûreté nucléaire, Bat 501, bois des Rames, 91400, Orsay, France

c Institut de Radioprotection et de Sûreté nucléaire, Cadarache Bat 153, 13108, St Paul-lès-Durance, France

1. Introduction

Anthropogenic radionuclides such as ^{137}Cs , plutonium isotopes and ^{241}Am in the environment of both hemispheres are mainly due to the 504 atmospheric nuclear weapons tests (NWTs), with a cumulated fission yield of 440 Mt, carried out worldwide between 1945 and 1980 (UNSCEAR, 2000). About 90% of radioactive debris in the Southern Hemisphere come from tests conducted in the Northern Hemisphere and the largest part (~ 85%) of ^{238}Pu is due to the dispersion of debris from a nuclear power generator SNAP-9A (SNAP) following its re-entry into the atmosphere of the Southern Hemisphere in 1964 (Krey, 1967; Hardy et al., 1972).

The global fallout (GF) of the ^{137}Cs ($T_{1/2}= 30.1$ yr.) in the Southern Hemisphere, as estimated from the total ^{90}Sr deposition weighted by the ratio of their fission yields, is 213 PBq (UNSCEAR, 2000). Assuming that the distribution of plutonium between both hemispheres is close to the distribution of ^{137}Cs , and that they have similar fallout histories, the cumulated GF in the Southern Hemisphere are of the order of 1.51 PBq, 1.01 PBq and 32.91 PBq for ^{239}Pu ($T_{1/2}=24,110$ yr.), ^{240}Pu ($T_{1/2}= 6,563$ yr.) and ^{241}Pu ($T_{1/2}= 14.35$ yr.), respectively. Assuming that the ^{241}Am ($T_{1/2}= 432.5$ yr.) is not formed during explosions and that it does not pre-exist in the explosive charge but that it comes totally from the decay of ^{241}Pu (Livingston et al., 1975, Krey et al., 1976), the cumulated quantity in 2018 would be 1.01 PBq. The ^{238}Pu inventory, from SNAP and NWTs, is estimated by soil sampling in 1970-71 at approximately 0.5 PBq (Hardy et al., 1973), mainly deposited on the ground in 1965. The maximum annual deposition of GF peaked in 1964 following the intensive United States (US) and former Soviet Union (FSU) tests in 1962. The average cumulative soil deposition between 1952 and 1980 peaked in 1963.

Between 1952 and 1958, United Kingdom (UK) conducted twelve conventional low-yield tests (total yield of 0.09 Mt) at three sites in Australia (Monte Bello, Emu, Maralinga) and three thermonuclear tests (0.3, 0.72 and 0.2 Mt) in the Malden Island (4°S - 155°W) leading to tropospheric injections of 0.096 and 0.56 Mt of fission energy, respectively. In 1957-1958, the UK carried out three thermonuclear tests (0.8 to 3 Mt) and two conventional tests (0.024 and 0.025 Mt) and in 1962 the US performed 24 tests (including 12 tests < 300 kt) at Christmas atolls (2°N - 157°W). Given the low latitude of the latter site, the USNCAER (2000) considers that the fission energy injected into the troposphere (3.62 Mt) has been evenly distributed between both hemispheres. From 1966 to 1974, France conducted forty-one atmospheric NWTs with a total yield of 10.1 Mt in the Southern Hemisphere: thirty-four tests (6.32 Mt) at Moruroa atoll, four tests (3.74 Mt) at Fangataufa atoll and three airdrops tests (0.064 Mt) over French territorial maritime in the vicinity of both atolls (22°S - 139°W) (Fig. 1). In addition, five safety trials were carried out in Moruroa for a total yield of 0.002 kt. The total yield for the ten thermonuclear devices ranged from 0.15 to 2.6 Mt and the thirty-one nuclear fusion devices did not exceed 0.45 Mt (24 below 100 kt and 7 from 100 to 450 kt). Fission products were distributed among the stratosphere (5.36 Mt), the troposphere (0.54 Mt) and in local-regional fallout (0.19 Mt). Local-regional fallout come from three barge tests in the lagoon of Moruroa (fission yield of 0.128 kt) in 1966-1967 and one barge test in the Fangataufa lagoon (0.0625 kt) carried out in 1966 (UNSCEAR, 2000). The main fallout in the Gambier archipelago come from these barge tests (Aldébarian of 02/07/1966 at Moruroa for a total yield of 24 kt and Rigel of 24/09/1966 at Fangataufa, 125 kt) but also some tests at altitude in balloons whose direct fallout are not classified as local fallout, as the Phoebé test of 08/08/71 at Moruroa, 4 kt (MINDEF, 2006; Drozdovitch et al., 2020). Based on the distribution between both hemispheres described in the compartmental atmospheric model (Bennett, 1978; UNSCEAR, 2000), stratospheric

injections from French tests in the Southern Hemisphere is 4.0 Mt (75% of stratospheric injections), compared to 36 Mt coming from atmospheric NWTs of the Northern Hemisphere, i.e. 11% (4.0 Mt/36.0 Mt) for ^{137}Cs fallout. Anthropogenic radioactive deposits in French Polynesia originate from the stratospheric fallout (GF) and close-in tropospheric fallout (LF) from French atmospheric testing. The average deposit of LF peaked in 1967.

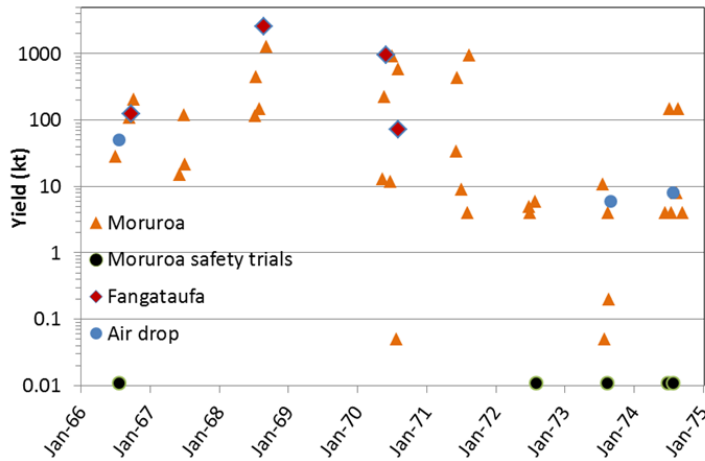


Fig. 1. Yield of atmospheric NWTs at Moruroa and Fangataufa and for airdrops (UNSCLEAR, 2000). Safety trials located at Moruroa are indicated by black points.

Nuclear measurements have been widely used in the past to determine the signature of a source, the origin and the contribution to NWTs fallout. This was the case, for example, to assess the contributions of the Chernobyl fallout (Mitchell et al., 1990; Holm et al. 1992; Pourcelot et al., 2003; Le Roux et al., 2010; Popov et al., 2010), or those of a nuclear industry (Charmasson et al., 1998; Duffa et al., 2001; Ueda et al., 2004; Gauthier-Lafaye et al., 2008). Mass spectrometry has been increasingly used in recent decades to supplement information; by having the advantage of direct access to accurate isotopic ratios, in particular with the atomic ratios of isotopes of heavy elements such as plutonium, to discern the local-regional fallout of a test site (Lindhahl et al., 2011; Tims et al., 2016; Buessler et al., 2018; Huang et al., 2019). This applies especially to the $(^{240}\text{Pu}/^{239}\text{Pu})_{\text{AR}}$, whose values have been widely characterized for various types of installation, accident or use of nuclear material (Mitchell et al., 1997; Warneke et al., 2002; Eriksson et al., 2008; Lindhal et al., 2010). $(^{241}\text{Pu}/^{239}\text{Pu})_{\text{AR}}$ as signatures, based on a direct ^{241}Pu measurement, are less frequent, they are often deduced by the measurement of its daughter ^{241}Am (Livingston et al., 1975; Koide et al., 1980).

In a previous study, we established inventories in ^{137}Cs , ^{238}Pu and $^{239+240}\text{Pu}$ on an island (Hiva Oa) in the Marquesas archipelago (Bouisset et al., 2018). This island is located at a latitude of only 10°S (139°W) more than 1,300 km north of both atolls of Moruroa and Fangataufa, and about 2,000 km southeast close to the Malden and Christmas Islands latitudes. In order to have additional data for Hiva Oa, that we consider as a reference site low affected by LF from French tests, we have made additional analysis in ^{241}Am activity concentration and $(^{240}\text{Pu}/^{239}\text{Pu})_{\text{AR}}$ atom ratio on some of our archived samples. These results are compared in this paper with those obtained in four of the main islands of the Gambier archipelago, located at 425 km southeast (23°S - 135°W) of the French test sites (Fig.2). This archipelago was the object of direct LF from French tests (MINDEF, 2006). The aims of the present study are to:

- establish signatures for test sites and GF. The signatures of the French tests sites can be deduced from activity concentrations measured in terrestrial samples in the framework of a radiological survey of both atolls carried out by international scientific teams coordinated by the IAEA (IAEA, 1998) and from plutonium atom ratios measured for some of these sample (Hrnecek et al., 2005). The GF signatures are derived from inventories published by UNSCEAR (2000) and data from soil samples collected in 1970 and 1971 as part of a GF evaluation program conducted by the US Department of Energy's Environmental Measurements Laboratory (EML) (Hardy et al., 1973; Kelley et al., 1999).
- carry out inventories in soils of the Gambier Islands for the ^{137}Cs , the isotopes of plutonium (238, 239 and 240) as well as the ^{241}Am .
- evaluate, from mixing equations of different isotopic ratios, the share of GF and the share of LF in Gambier and Hiva Oa.
- propose the specific signatures of the stratospheric fallout in the Southern Hemisphere formed partly by those of the Northern Hemisphere and partly by those of the injections of the French tests.

2. Materials and methods

2.1 *Sample collection and preparation*

Soils core have been collected in four islands of the Gambier archipelago in May 2018 and in one island of the Marquesas in the archipelago in August 2016. The Gambier archipelago consists of four main islands, the most populated of which is Mangareva, where the highest peak's altitude is 441 m. Four samples were taken in the main island and three in small islands, Aukena, Akamaru and Taravai, (Table 1, Fig. 2). The mean annual rainfall amounts recorder from 1969 to 1974 in Gambier (meteorological station at Totogegie motu) was 1352 ± 224 mm, ranging from 987 to 1544 mm. No information were available on precipitation frequency and no data outside this period. The Marquesas archipelago consists of fourteen islands, one of the most populated is Hiva Oa, where the highest peak is at 1230 m. Sampling was conducted in 2016 at five sites (Table 1, Fig. 2). Mean annual rainfall amounts recorder from 1954 to 1980 was 1126 ± 350 mm ranging from 561 to 1896 mm. During the same period, the average precipitation frequency was 179 ± 41 d.yr⁻¹. The selected sites were in relatively flat areas in order to limit run-off erosion. Their choice was also based on an accessibility, distance from roads and dwellings, and reasonable assurance that the soil had remained undisturbed since the 1960s. Seven and five sites were selected at Gambier Islands and at Hiva Oa respectively. The number of sites was reduced by one site for each of both islands (sample id. Ga4 and Hv3) as activity measurements indicated that these sites had been recently disturbed. At each site, 30-cm (Hiva Oa) and 45-cm (Gambier Islands) deep soil samples were collected in two/three successive procedures (0-15 cm, 15-30 cm and 30-45cm) using an 8-cm diameter corer in three locations about three meters apart. Greater depth was sampled for Gambier sites as our preliminary study in 2014 showed higher concentrations in soils in this archipelago.

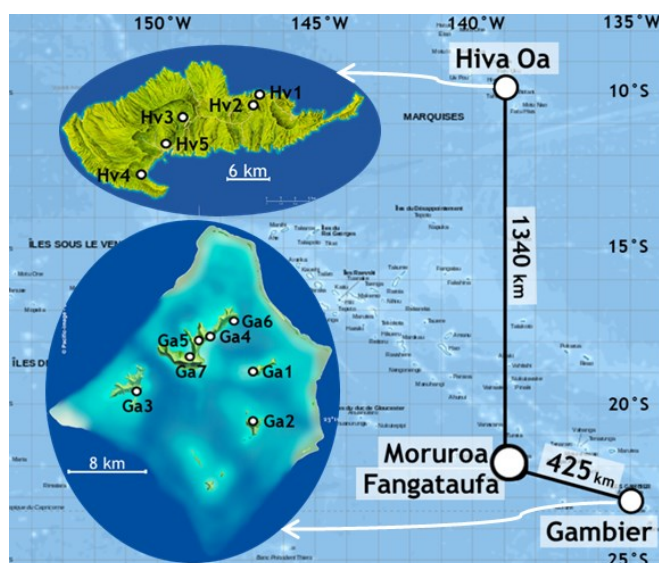


Fig. 2. Location of soil sampling sites at Hiva Oa and Gambier Islands and location of these islands and French test sites of Moruroa and Fangataufa in French Polynesia.

Table 1 Sample location, core density and loss of ignition.

Archipelago Island (Sampling date)	Area (km ²)	Sample Id.	GPS coordinates (W and S)		Altitude (m ASL ^a)	Average core density (g.cm ⁻³)		LOI 550°C (%)
						Raw	Processed	
Marquesas	997							
Hiva Oa (August 2016)	316	Hv1	138°55'33.3"	09°44'15.0"	46	1.25	1.08	7.5-13
		Hv2	138°55'53.3"	09°45'23.5"	425	1.04	1.04	10-22
		Hv3	139°00'37.1"	09°45'42.1"	494	1.08	0.90	20-29
		Hv4	139°04'14.4"	09°49'56.0"	139	1.04	0.98	11-20
		Hv5	139°02'16.5"	09°47'41.6"	193	1.24	1.23	11-15
Gambier	31							
Aukena Akamaru Taravai Mangareva (May 2018)	1.35	Ga1	134°54'58.4"	23°08'13.4"	22	0.97	0.89	7.8-22
		Ga2	134°54'48.4"	23°10'57.0"	49	1.04	0.98	13-26
		Ga3	135°02'01.6"	23°09'18.7"	24	0.93	0.92	12-26
	15.4	Ga4	134°57'32.7"	23°06'00.7"	76	0.81	0.81	11-19
		Ga5	134°58'20.0"	23°06'18.8"	42	0.97	0.95	12-23
		Ga6	134°56'00.2"	23°05'28.1"	21	0.97	0.95	10-33
		Ga7	134°58'37.2"	23°07'25.8"	103	1.14	1.08	9.0-27

The preparation is identical to that used in our previous study (Bouisset et al., 2018). Briefly, each core sample was divided into 2-cm thick layers for depths between 0 and 10 cm and into 5-cm thick layers for depths up to 30 cm at Hiva Oa or up to 45 cm at Gambier. The corresponding layers for the three sampling site were grouped together and dried at 60°C for three days. The mass of water in these soils range 30-65% of the raw mass. Roots and large stones were removed and the samples were ground. For the raw dry soils, the densities were on average 1.13 at Hiva Oa and 0.98 at Gambier. The average density of the processed soil samples was respectively 1.05 and 0.94 at the same islands. The average density (Table 1), coarse particles removed, of each core (0-30/45 cm)

which is used to calculate the inventories. The loss of ignition (LOI) between 60°C and 550°C was determined as the arithmetic mean of the mass differences of the dry and ash samples for five aliquots of about 5 g DW. Organic contents of the soils, as showed in LOI, are roughly the same in Hiva Oa and Gambier with 20%-30% surface contents and 10% depth contents, except for the recently disturbed Hv3 and Ga4 sites where the contents vary little with depth. Depending on the quantities of soil available, cylindrical polyethylene counting containers of 200 mL (layers 0-10 cm) or 380 mL (layers 10-45 cm) were filled in to be measured by gamma spectrometry, while about 50 g were dedicated for measurements by alpha spectrometry and Inductively coupled mass spectrometry (ICPMS). The Hv3 and Ga4 sites, whose low concentrations measured in all layers confirm that these soils have been altered, were excluded from our study.

2.2 Measurements

Gamma-ray spectrometry was performed to quantify the ^{137}Cs activities in all layers. Counting times ranged from one to five days to measure ^{137}Cs concentrations up to approximately 0.1 Bq.kg^{-1} and to reduced statistical uncertainty to less than 10% for activities above 0.3 Bq.kg^{-1} . Measurements were made using a high purity Ge (HPGe) detector (56% relative efficiency). Detailed of the electronic chains and calibrations procedure were described previously (Bouisset and Calmet, 1997; Bouisset et al., 2018). Multi-gamma Analytics sources, in the same container that those used for sample measurements, are used for efficiency calibrations in the energy range 46 keV-2.5 Mev, taking account for self-absorption effects and scheme summations.

The determination of all isotopes of plutonium at very low level of radioactivity is done in two steps. The first ones uses radioactive properties of the radioisotopes and allows to quantify by alpha spectrometry ^{238}Pu , $^{239+240}\text{Pu}$ and ^{241}Am , after a high chemical purification of a large amount of sample (about 50 g of dry soil in this study). This analysis is made according to the standard NF ISO 18589-4. The second step is based on the atomic properties of plutonium isotopes and allows to quantify by ICP-MS SF ^{239}Pu , ^{240}Pu and ^{241}Pu . For the “alpha spectrometry protocol”, the quality of the chemical reagents are for Analysis (ACS) and for the “ICP-MS protocol” the reagents are Suprapur quality. Control blanks and reference materials are regularly carried out to ensure the quality of the analyses.

First step - After drying and calcination of the samples, about 50 g of dry soils are taken and spiked with ^{242}Pu (NIST SRM 4334) and ^{243}Am (NPL A14063). The sample is leached with hot acid attack in an open system with concentrated HNO_3 , H_2O_2 and HCl . To remove a part of the matrix, three successive coprecipitations of actinides are done (two calcium oxalate and an iron hydroxide). Pu(IV) and Am(III) are separated by using a chromatography column with anion exchange resin AG1X8 (Bio-rad), conditioned in 8M HNO_3 . After loading and washing with 8M HNO_3 , the solution is preserved for the purification of the Am fraction. Pu is then eluted with 12M $\text{HCl}/0.1\text{M NH}_4\text{I}$. Three successive chromatography columns are performed to purify the Am fraction : AG1X8/AG50W (Bio-rad) to separate Am from (Fe, U, Th) ; TRU resin (Triskem) to separate Am from (Cu, Ni) and AG1X4 resin (Bio-rad) to separate Am from the rare earth elements. The purified fractions containing Pu and Am are evaporated, then the residues are dissolved in concentrated HNO_3 and diluted. Both sources are prepared by electrodeposition onto stainless steel discs as the cathode, Pt as the anode. Pu and Am isotopes are measured by a low level background alpha spectrometer (alpha-analyst, Canberra) with 450 mm^2 PIPS detectors and using Genie 2000 software (Canberra). The counting time is fourteen days to obtain a very low level of activity.

Second step - After the measurement by alpha spectrometry, recover the Pu electroplated sample with concentrated HNO₃ and HCl. Evaporate to dryness, then dissolve it with 8M HNO₃. Add NaNO₂ to get Pu(IV). Purify the sample on anion exchange resin AG1X8 (Dowex) with 8M HNO₃ as fixing medium and concentrated HCl/HI as elution medium. Evaporate to dryness then recovery in 0,5M HNO₃ for measurement by ICP-MS Sector Field (Element 2, ThermoFisher Scientific). The introduction system is composed of a PFA MicroFlow nebulizer (200 μL/min) connected to a high sensitivity desolvating system (apex Ω, ESI) and a cyclonic spray chamber (PC3 - ESI). A high capacity dry interface pump and a specially designed set of cones (Jet Interface) are used to increase the sensitivity of the signal. The quantification is done by isotopic dilution using the ²⁴²Pu tracer added at the beginning of the analysis.

The measurements of plutonium by alpha spectrometry were carried out by two different laboratories of the Institute of Radiation Protection and Nuclear Safety (IRSN). Those of Hiva Oa and sections 30-45 cm of Gambier were carried out by the Laboratory for the Study and Monitoring of the Environment (LESE) with the protocol detailed in (Bouisset et al., 2018) and those of the 0-30 cm of Gambier were carried out by the Laboratory of Radioactivity Measurement in the Environment (LMRE) with the protocol described above. In order to verify the consistency of the measurements of both laboratories, a sample (layer 4-6 cm) of each of the four Hiva Oa sites was again measured by the LMRE by quantifying plutonium (Fig. 3) in addition to ²⁴¹Am.

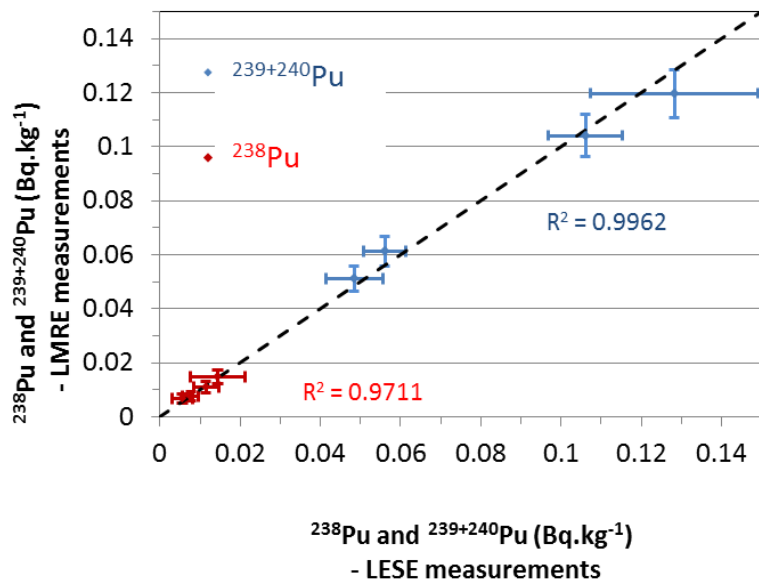


Fig. 3. ²³⁸Pu and ²³⁹⁺²⁴⁰Pu concentrations measured by the two IRSN laboratories (LMRE and LESE) in Hiva Oa soils (layer 4-6 cm).

2.3 Two end-member model

This model is a very sensitive method to determine the share of fallout from two sources. It was used in the 1970s to distinguish the proportion of plutonium from GF from that of the nuclear industry (Krey et al., 1976). Any isotopic ratio R_m measured on a site, where the fallout comes from two source terms with different R_1 and R_2 signatures can be written:

$$R_m = x_1 R_1 + (1 - x_1) R_2$$

where x_1 et $1-x_1$ are contributions from both sources giving the mixing equation :

$$X_1 = \frac{(R_m - R_2)}{(R_1 - R_2)} \quad (1)$$

If another isotopic ratio R'_m is determined, with R'_1 and R'_2 characteristic signatures of both sources, then:

$$\frac{(R'_m - R'_2)}{(R'_1 - R'_2)} = \frac{(R_m - R_2)}{(R_1 - R_2)}$$

hence the mixing equation of a two end-member model:

$$R'_m = A + B R_m \quad (2)$$

with $B = \frac{(R'_1 - R'_2)}{(R_1 - R_2)}$ and $A = R'_2 - B R_2$

The coordinates of the two ends of Eq. (2) are the isotopic ratio pairs (R_1, R'_1) and (R_2, R'_2) . The measure at point (R_m, R'_m) is on this mixing line if there are really only two source terms. The two end-member model was used to discern the global stratospheric fallout from the tropospheric fallout due to the French tests in the south-equatorial region (0-30°S) (Kelley et al., 1999). If one of the two source terms, the one with the signatures (R_1, R'_1) for example, is itself made up of two other source terms (R_{1-1}, R'_{1-1}) and (R_{1-2}, R'_{1-2}) , a second mixing equation can be written:

$$R'_1 = A_1 + B_1 R_1 \quad (3)$$

with $B_1 = \frac{(R'_{1-1} - R'_{1-2})}{(R_{1-1} - R_{1-2})}$ et $A_1 = R'_{1-2} - B_1 R_{1-2}$

The coordinates of the intersection of the two mixing lines Eq. (2) and Eq. (3) correspond to the signatures (R_1, R'_1) of the mixing of both sources such as:

$$R_1 = \frac{A - A_1}{B_1 - B} \quad \text{et} \quad R'_1 = B R_1 + A \quad (4)$$

3. Results

Table 2 shows the ^{137}Cs , plutonium isotopes and ^{241}Am activity concentrations ($\text{Bq} \cdot \text{kg}^{-1}$ DW, decay corrected at May 2018) and the $(^{240}\text{Pu}/^{239}\text{Pu})_{\text{AR}}$ for all measured layers in Gambier Islands and in Table 3 for Hiva Oa Island. The uncertainties at 2σ include statistical counting and calibration errors. The first section of the third core (30-35 cm) from the Gambier sites, with the exception of Ga7, was found to be contaminated with surface debris when the core sampler was re-introduced. These results were excluded from Table 2.

Table 2

Concentrations of ^{137}Cs , ^{238}Pu , $^{239+240}\text{Pu}$, ^{241}Am , and $(^{240}\text{Pu}/^{239}\text{Pu})_{\text{AR}}$ in core soils of Gambier Islands, in 2018.

Island (sample Id.)	Depth ($\text{g} \cdot \text{cm}^{-2}$)	Activity concentration ($\text{Bq} \cdot \text{kg}^{-1}$ DW)				Atom ratio
		^{137}Cs	^{238}Pu	$^{239+240}\text{Pu}$	^{241}Am	($^{240}\text{Pu}/^{239}\text{Pu}$) _{AR}
Aukena (Ga1)	0-1.4	4.31 ± 0.26	0.0399 ± 0.0047	0.827 ± 0.035	0.0728 ± 0.0054	0.0394 ± 0.0063
	1.4-3.1	4.11 ± 0.25	0.0431 ± 0.0050	0.849 ± 0.043	0.0706 ± 0.0051	0.0367 ± 0.0031
	3.1-4.8	3.73 ± 0.22	0.0390 ± 0.0037	0.703 ± 0.030	0.0663 ± 0.0043	0.0381 ± 0.0040
	4.8-6.6	3.42 ± 0.21	0.0345 ± 0.0039	0.616 ± 0.026	0.0595 ± 0.0049	0.0403 ± 0.0032
	6.6-8.2	3.17 ± 0.20	0.0359 ± 0.0036	0.690 ± 0.029	0.0608 ± 0.0042	0.0370 ± 0.0040
	8.2-12.4	2.09 ± 0.14	0.0300 ± 0.0037	0.642 ± 0.030	0.0527 ± 0.0042	0.0350 ± 0.0031
	12.4-17.1	1.200 ± 0.084	0.0128 ± 0.0021	0.244 ± 0.013	0.0301 ± 0.0027	0.0461 ± 0.0046
	17.1-22.2	0.350 ± 0.036	0.0059 ± 0.0015	0.1110 ± 0.0080	0.0103 ± 0.0017	0.0413 ± 0.0031
	22.2-27.0	0.130 ± 0.020	0.0032 ± 0.0010	0.0520 ± 0.0040	0.0046 ± 0.0010	0.0365 ± 0.0062
	32.0-36.5	0.043 ± 0.014	0.00145 ± 0.00089	0.0093 ± 0.0022		

	36.5-41.5	0.0115 ± 0.0085				
Akamaru (Ga2)	0-1.4	2.16 ± 0.15	0.0462 ± 0.0041	0.801 ± 0.030	0.0596 ± 0.0054	0.0313 ± 0.0024
	1.4-3.1	2.28 ± 0.16	0.0387 ± 0.0037	0.850 ± 0.034	0.0549 ± 0.0050	0.0318 ± 0.0025
	3.1-4.6	2.32 ± 0.15	0.0400 ± 0.0052	0.707 ± 0.038	0.0468 ± 0.0039	0.0325 ± 0.0036
	4.6-6.1	2.38 ± 0.16	0.0362 ± 0.0038	0.716 ± 0.028	0.0478 ± 0.0053	0.0320 ± 0.0026
	6.1-7.6	2.37 ± 0.16	0.0352 ± 0.0041	0.623 ± 0.030	0.0502 ± 0.0043	0.0342 ± 0.0036
	7.6-12.0	2.24 ± 0.15	0.0409 ± 0.0039	0.777 ± 0.035	0.0520 ± 0.0050	0.0308 ± 0.0026
	12.0-17.2	2.17 ± 0.14	0.0343 ± 0.0031	0.538 ± 0.022	0.0440 ± 0.0042	0.0348 ± 0.0035
	17.2-22.1	1.74 ± 0.12	0.0234 ± 0.0030	0.428 ± 0.020	0.0330 ± 0.0037	0.0352 ± 0.0039
	22.1-26.9	1.046 ± 0.060	0.0115 ± 0.0021	0.236 ± 0.014	0.0207 ± 0.0029	0.0372 ± 0.0031
	32.5-38.1	0.226 ± 0.029	0.0030 ± 0.0011	0.0259 ± 0.0044		
	38.1-44.0	0.094 ± 0.020	0.0016 ± 0.0013	0.0135 ± 0.0023		
	Taravai (Ga3)	0-1.5	1.81 ± 0.14	0.0376 ± 0.0040	0.456 ± 0.021	0.0427 ± 0.0037
2.5-3.3		2.06 ± 0.14	0.0310 ± 0.0032	0.404 ± 0.020	0.0405 ± 0.0039	0.0402 ± 0.0034
3.3-5.0		2.31 ± 0.15	0.0278 ± 0.0028	0.368 ± 0.018	0.0392 ± 0.0040	0.0400 ± 0.0038
5.0-6.8		2.19 ± 0.15	0.0304 ± 0.0033	0.443 ± 0.020	0.0436 ± 0.0045	0.0379 ± 0.0033
6.8-8.7		1.94 ± 0.13	0.0306 ± 0.0028	0.414 ± 0.019	0.0467 ± 0.0061	0.0401 ± 0.0038
8.7-14.0		1.64 ± 0.12	0.0285 ± 0.0032	0.380 ± 0.018	0.0341 ± 0.0040	0.0372 ± 0.0027
14.0-18.5		1.182 ± 0.063	0.0167 ± 0.0021	0.237 ± 0.012	0.0264 ± 0.0038	0.0416 ± 0.0036
18.5-23.0		0.779 ± 0.060	0.0081 ± 0.0019	0.1154 ± 0.0087	0.0207 ± 0.0028	0.0513 ± 0.0067
23.0-27.2		0.497 ± 0.043	0.0049 ± 0.0013	0.0773 ± 0.0060	0.0119 ± 0.0024	0.0539 ± 0.0044
31.9-36.7		0.143 ± 0.024	0.0028 ± 0.0012	0.0259 ± 0.0044		
36.7-41.6		0.074 ± 0.020	0.0012 ± 0.0007	0.0135 ± 0.0023		
Mangareva (Ga5)		0-1.5	2.39 ± 0.16	0.0424 ± 0.0043	0.836 ± 0.033	0.0680 ± 0.0054
	1.5-2.9	2.65 ± 0.18	0.0445 ± 0.0042	0.793 ± 0.036	0.0656 ± 0.0068	0.0368 ± 0.0028
	2.9-4.4	2.99 ± 0.19	0.0464 ± 0.0046	0.873 ± 0.034	0.0892 ± 0.0075	0.0384 ± 0.0029
	4.4-5.9	3.15 ± 0.20	0.0445 ± 0.0043	0.817 ± 0.031	0.0752 ± 0.0061	0.0364 ± 0.0031
	5.9-7.8	2.82 ± 0.17	0.0561 ± 0.0063	0.991 ± 0.040	0.0938 ± 0.0079	0.0355 ± 0.0036
	7.8-13.2	2.14 ± 0.14	0.0288 ± 0.0033	0.545 ± 0.024	0.0590 ± 0.0063	0.0435 ± 0.0038
	13.2-17.8	1.35 ± 0.10	0.0131 ± 0.0020	0.239 ± 0.012	0.0423 ± 0.0069	0.0535 ± 0.0054
	17.8-22.2	0.818 ± 0.058	0.0070 ± 0.0015	0.1017 ± 0.0074	0.0166 ± 0.0035	0.0641 ± 0.0064
	22.2-26.5	0.552 ± 0.045	0.0049 ± 0.0014	0.0904 ± 0.0079	0.0122 ± 0.0026	0.0464 ± 0.0035
	30.9-35.8	0.193 ± 0.026	0.0016 ± 0.0010	0.0550 ± 0.0042		
	35.8-40	0.146 ± 0.025	0.00079 ± 0.00068	0.042 ± 0.022		
	Mangareva (Ga6)	0-1.6	2.25 ± 0.15	0.0353 ± 0.0039	0.804 ± 0.032	0.0408 ± 0.0049
1.6-3.1		2.48 ± 0.17	0.0306 ± 0.0031	0.652 ± 0.029	0.0333 ± 0.0044	0.0274 ± 0.0024
3.1-4.8		2.51 ± 0.17	0.0418 ± 0.0045	0.967 ± 0.038	0.0455 ± 0.0060	0.0259 ± 0.0026
4.8-6.7		2.57 ± 0.16	0.0393 ± 0.0035	0.880 ± 0.036	0.0350 ± 0.0057	0.0260 ± 0.0022
6.7-8.5		2.42 ± 0.16	0.0421 ± 0.0054	0.917 ± 0.037	0.0376 ± 0.0056	0.0268 ± 0.0023
8.5-13.3		1.91 ± 0.11	0.0275 ± 0.0033	0.472 ± 0.022	0.0328 ± 0.0048	0.0350 ± 0.0032
13.3-17.6		1.200 ± 0.073	0.0190 ± 0.0031	0.345 ± 0.019	0.0229 ± 0.0040	0.0315 ± 0.0032
17.6-22.2		0.666 ± 0.053	0.0115 ± 0.0023	0.1173 ± 0.0096	0.0145 ± 0.0033	0.0476 ± 0.0039
22.2-27.1		0.571 ± 0.048	0.00181 ± 0.00074	0.0366 ± 0.0037	0.0140 ± 0.0034	0.101 ± 0.011
32.6-37.5		0.050 ± 0.018	0.00041 ± 0.00063	0.00766 ± 0.00018		
37.5-42.7		0.031 ± 0.019				
Mangareva (Ga7)		0-1.2	2.34 ± 0.17	0.0228 ± 0.0036	0.353 ± 0.021	0.0450 ± 0.0043
	1.2-2.8	2.33 ± 0.16	0.0225 ± 0.0031	0.347 ± 0.018	0.0522 ± 0.0044	0.0531 ± 0.0046
	2.8-4.6	2.38 ± 0.16	0.0260 ± 0.0035	0.352 ± 0.019	0.0508 ± 0.0044	0.0528 ± 0.0047
	4.6-6.5	2.43 ± 0.15	0.0219 ± 0.0024	0.310 ± 0.015	0.0434 ± 0.0044	0.0537 ± 0.0039
	6.5-8.6	2.28 ± 0.15	0.0219 ± 0.0034	0.317 ± 0.018	0.0494 ± 0.0045	0.0535 ± 0.0046
	8.6-14.4	2.15 ± 0.14	0.0205 ± 0.0025	0.295 ± 0.014	0.0393 ± 0.0042	0.0523 ± 0.0041
	14.4-19.9	1.86 ± 0.12	0.0179 ± 0.0032	0.237 ± 0.015	0.0377 ± 0.0039	0.0555 ± 0.0047
	19.9-26.1	1.264 ± 0.077	0.0125 ± 0.0017	0.160 ± 0.010	0.0228 ± 0.0030	0.0580 ± 0.0053
	26.1-32.1	0.750 ± 0.050	0.0096 ± 0.0019	0.1078 ± 0.0088	0.0165 ± 0.0021	0.0553 ± 0.0050
	32.1-38.0	0.502 ± 0.051	0.0041 ± 0.0014	0.0725 ± 0.0060		
	38.0-43.4	0.237 ± 0.029	0.0022 ± 0.0012	0.0273 ± 0.0038		
	43.4-48.5	0.081 ± 0.019				

Table 3

$^{239+240}\text{Pu}$ concentrations (Bouisset et al., 2018), ^{241}Am concentrations and $(^{240}\text{Pu}/^{239}\text{Pu})_{\text{AR}}$ measured in Hiva Oa soils in 2018

Sample Id.	Depth (g.cm ⁻²)	Activity concentration (Bq.kg ⁻¹ DW)		Atom ratio (at./at.) ($^{240}\text{Pu}/^{239}\text{Pu})_{\text{AR}}$
		$^{239+240}\text{Pu}$	^{241}Am	
Hv1	4-6	0.0484 ± 0.0071	0.0205 ± 0.0036	0.154 ± 0.013
	8-10	0.0318 ± 0.0032		0.149 ± 0.019
	10-15	0.0199 ± 0.0034		0.157 ± 0.014

Hv2	4-6	0.128 ± 0.021	0.0416 ± 0.0083	0.129 ± 0.012
	8-10	0.074 ± 0.015		0.141 ± 0.033
	10-15	0.0447 ± 0.0054		0.159 ± 0.016
Hv4	4-6	0.1061 ± 0.0091	0.0435 ± 0.0074	0.143 ± 0.011
	8-10	0.0759 ± 0.0130		0.154 ± 0.015
	10-15	0.0543 ± 0.0063		0.133 ± 0.013
Hv5	4-6	0.0560 ± 0.0052	0.0195 ± 0.0061	0.127 ± 0.011
	8-10	0.0442 ± 0.0049		0.132 ± 0.011
	10-15	0.0497 ± 0.0056		0.129 ± 0.021

4. Discussion

4.1 Signatures of test sites

Activity ratios (Table 5) can be derived from results in terrestrial samples (top soils, coral bedrocks and loose coral rocks) collected in 1996 at Moruroa and Fangataufa (IAEA, 1998). The isotopic ratios reported below are decay corrected to 2018 and expressed with a measurement uncertainty at 2 σ . The only fission products sometimes detected in these samples are ^{137}Cs and ^{90}Sr . The activity concentrations of ^{137}Cs are low, often less than 1 Bq.kg^{-1} , as noted several times (IAEA, 1998; Danesi et al., 2002; MINDEF, 2006; DSCEN, 2013). The ^{90}Sr measurement was carried out on some of the samples. Fig 4 shows the ^{90}Sr activity concentrations vs $^{239+240}\text{Pu}$ activity concentrations for the top soils. ^{137}Cs is derived from ^{90}Sr , corrected for its decay in 1967, by the $^{137}\text{Cs}/^{90}\text{Sr}$ fission ratio of 1.5 (UNSCEAR, 2000). The average activity ratio $^{137}\text{Cs}/^{239+240}\text{Pu}$, in 2018, is 0.51 ± 0.06 ($n = 4$; range 0.36-0.67) at Fangataufa. For Moruroa, two very distinct sets of results give average activity ratios of 0.08 ± 0.03 ($n = 4$; range 0.02-0.12) and 0.005 ± 0.005 ($n = 11$; range 0.003-0.009). This variability of results, twelve from one site and three from a second site, must be related to the type of the soil, consisting mainly of coral with varying organic matter content. The highest set of ratios is therefore probably the closest to the Moruroa site signature. For both test sites, the ratios obtained can only be considered as minimum values of their signatures. The plutonium isotopes and ^{241}Am concentrations are higher and the activity ratios between these radionuclides are relatively homogeneous on each of both atolls. The activity ratios are calculated for the samples with $^{239+240}\text{Pu}$ concentrations greater than 50 Bq.kg^{-1} so that the reciprocal fallout from both test sites does not interfere, as well as those of SNAP for ^{238}Pu . Fig. 4 shows ^{238}Pu activity concentrations vs $^{239+240}\text{Pu}$ activity concentrations of the all sample measurements in both atolls. ^{238}Pu and $^{239+240}\text{Pu}$ concentrations are linearly correlated for $^{239+240}\text{Pu} > 50 \text{ Bq.kg}^{-1}$, leading to average $^{238}\text{Pu}/^{239+240}\text{Pu}$ activity ratios of 0.0052 ± 0.0026 ($n = 40$; range 0.004-0.017) at Moruroa and 0.325 ± 0.039 ($n = 9$, range 0.30-0.37) at Fangataufa. These activity ratios are representative of four sites around the Moruroa atoll and two sites in the northeast and east of the Fangataufa atoll. Activity ratios close to those from Moruroa were found in the vicinity of the Nevada Site Test (NTS) where low yield NWTs (1951-1958) and safety tests (1955-1963) have been conducted. At Queen City Summit, located 50 km north of NTS, the $^{238}\text{Pu}/^{239+240}\text{Pu}$ ratio is of 0.011 ± 0.002 (decay corrected to 2018) at the ground surface, lower than those in depth due to recent addition of wind-borne soil from NTS (Turner et al., 2003). ^{241}Am vs $^{239+240}\text{Pu}$ measured in the samples of both atolls are reported in Fig. 4. The average $^{241}\text{Am}/^{239+240}\text{Pu}$ ($^{239+240}\text{Pu} > 50 \text{ Bq.kg}^{-1}$) is 0.025 ± 0.008 ($n = 38$, range 0.01-0.06) at Moruroa and 0.070 ± 0.012 ($n = 8$, range 0.06-0.09) at Fangataufa. Since ^{241}Pu is not directly measured, its activity is deducted from that of its daughter ^{241}Am , assuming that the latter does not pre-exist in the fuel before the explosion (Krey et al., 1976; Varga, 2007): $^{241}\text{Am}(t_0)=0$. If t_1 is the date of the measurement of $^{241}\text{Am}(t_1)$, the filiation of both radionuclides makes it possible to calculate at the date t_2 the activity in $^{241}\text{Pu}(t_2)$ with the following relation:

$${}^{241}\text{Pu}(t_2) = \frac{{}^{241}\text{Am}(t_1)(T_2 - T_1)}{T_1 \left(e^{-\text{Ln}(2)\left(\frac{t_1}{T_2} - \frac{t_2}{T_1}\right)} - e^{-\text{Ln}(2)\frac{t_1 - t_2}{T_1}} \right)} \quad (5)$$

where T_1 and T_2 are the half-life of ${}^{241}\text{Pu}$ and ${}^{241}\text{Am}$ respectively.

The average ${}^{241}\text{Pu}/{}^{239+240}\text{Pu}$ activity ratio calculated applying Eq. (5) are of 0.074 ± 0.022 (0.03-0.18) at Moruroa and 0.209 ± 0.037 (0.18-0.25) at Fangataufa. Similar values were reported for sites where low-yield atmospheric tests have been conducted, such as Semipalatinsk-USSR (0.054) or Emu and Maralinga - Australia (0.03-0.04) (Irlweck and Hrnccek, 1999), decay corrected to 2018. Measurements of $({}^{240}\text{Pu}/{}^{239}\text{Pu})_{\text{AR}}$ were made for some of the samples collected by the IAEA in 1996, leading to values of 0.018 ± 0.005 at Moruroa and 0.049 ± 0.001 at Fangataufa (Hrnccek et al., 2005), in the same range as the values measured in lagoon sediments (Chiappini et al., 1996; Chiappini et al., 1999). These low ratios are characteristic of low yield nuclear detonations (Krey et al., 1976). They are close to those measured, about 0.03-0.06, in the vicinity of the UK-test areas (Maralinga, Monte-Bello) in Australia (Tims et al., 2013; Johansen et al., 2014) or at Enewatak atoll (Muramatsu et al., 2001; Buessler et al., 2018). From these activity ratios and $({}^{240}\text{Pu}/{}^{239}\text{Pu})_{\text{AR}}$ we deduce the $({}^{241}\text{Pu}(t)/{}^{239}\text{Pu})_{\text{AR}}$ with the following relation:

$$\left(\frac{{}^{241}\text{Pu}(t)}{{}^{239}\text{Pu}} \right)_{\text{AR}} = \frac{{}^{241}\text{Pu}(t)}{{}^{239+240}\text{Pu}} \left(\frac{T_1}{T_4} + \frac{T_1}{T_3} \left(\frac{{}^{240}\text{Pu}}{{}^{239}\text{Pu}} \right)_{\text{AR}} \right) \quad (6)$$

where T_3 and T_4 are the half-life of ${}^{240}\text{Pu}$ and ${}^{239}\text{Pu}$ respectively.

The $({}^{241}\text{Pu}/{}^{239}\text{Pu})_{\text{AR}}$ are $(0.47 \pm 0.20)10^{-4}$ $[(0.21 - 1.2) 10^{-4}]$ at Moruroa and $(1.47 \pm 0.26)10^{-4}$ $[(1.2 - 1.8) 10^{-4}]$ at Fangataufa.

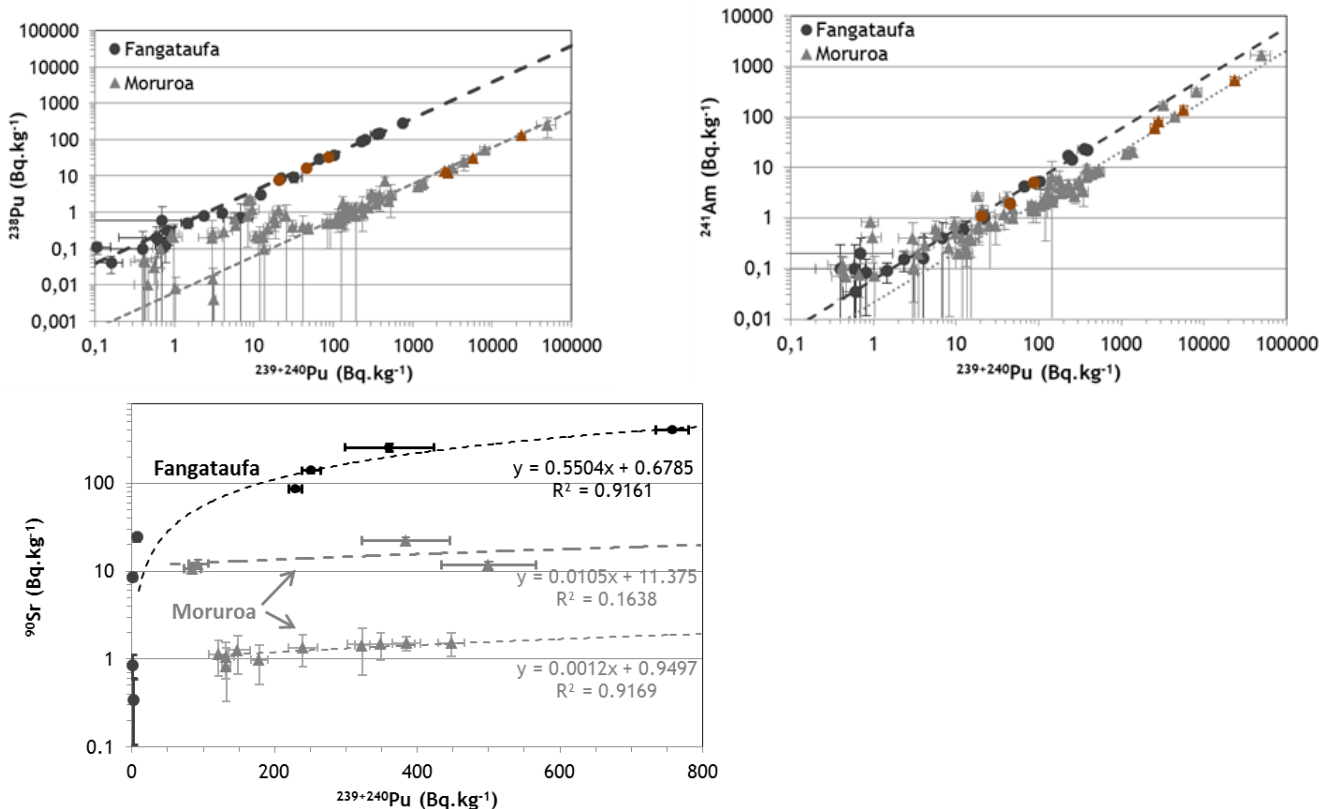


Fig. 4. Activity concentrations of ^{238}Pu , ^{241}Am and ^{90}Sr vs $^{239+240}\text{Pu}$, in 1996, for soil samples at Moruroa and Fangataufa (IAEA, 1998). Dotted lines indicate the mean values for samples with $^{239+240}\text{Pu}$ concentrations greater than 50 Bq.kg^{-1} . Mean $(^{240}\text{Pu}/^{239}\text{Pu})_{\text{AR}}$ was determined for samples with activities indicated in brown (Hrnecek et al., 2005).

4.2 Signatures of GF

Assuming that the fallout distribution of plutonium and fission products has been identical between the two hemispheres, the global activity ratios in 2018 are 24.4 in $^{137}\text{Cs}/^{239+240}\text{Pu}$, 0.98 in $^{241}\text{Pu}/^{239+240}\text{Pu}$ and the atom ratios are 0.182 in $(^{240}\text{Pu}/^{239}\text{Pu})_{\text{AR}}$ and $9.7 \cdot 10^{-4}$ in $(^{241}\text{Pu}/^{239}\text{Pu})_{\text{AR}}$. The $^{241}\text{Am}/^{239+240}\text{Pu}$ activity ratio is 0.38 in 2018, calculating ^{241}Am based on the radioactive decay from the annual ^{241}Pu fallout (Fig. 5) and considering an average stratospheric residence time of about one year (Krey et al., 1970; Koide et al., 1979). The $^{241}\text{Am}/^{239+240}\text{Pu}$ activity ratio thus calculated in 1970 is 9.4, which corresponds to the value reported for samples measured that year in the Northern Hemisphere ($22^\circ\text{N} - 60^\circ\text{N}$) (Livingston et al. 1975). $(^{240}\text{Pu}/^{239}\text{Pu})_{\text{AR}}$ of 0.173 ± 0.027 and $(^{241}\text{Pu}/^{239}\text{Pu})_{\text{AR}}$ of $(7.25 \pm 2.52) \cdot 10^{-4}$ are the values obtained from the measurement of soils collected by the EML in 1970-1971 in the $0\text{-}30^\circ\text{S}$ latitude range (Kelley et al., 1999). The $^{238}\text{Pu}/^{239+240}\text{Pu}$ activity ratio from NWTs GF has been estimated at 0.016 ± 0.004 . Taking into account the fallout of SNAP, the $^{238}\text{Pu}/^{239+240}\text{Pu}$ activity ratio of GF in the Southern Hemisphere is 0.12 ± 0.04 on average, variable with latitude (Hardy et al., 1973).

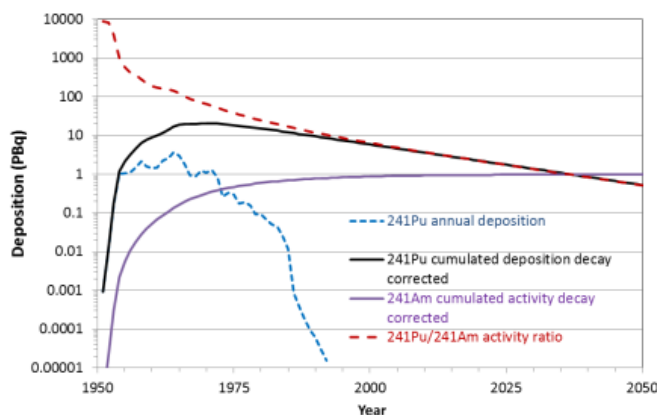


Fig. 5. Annual cumulative deposition of ^{241}Pu in the Southern Hemisphere derived from ^{137}Cs (UNSCEAR, 2000), annual ingrowth cumulated of ^{241}Am and $^{241}\text{Pu}/^{241}\text{Am}$ activity ratio.

4.3 Inventories in Gambier

Concentrations of radionuclides as a function of depth decrease exponentially beyond a certain depth x according to the relation $C(x) = a e^{-\alpha x}$, where a is the activity concentration at the ground surface ($x=0 \text{ g.cm}^{-2}$) and α the relaxation coefficient of the exponential function, in $\text{g}^{-1}.\text{cm}^2$ (Schuller et al., 2002; Bouisset et al., 2018). For the first section of the third core of five of the six sites, contaminated with surface debris as noted above, concentrations are derived from the exponential relationship. The propagation of these exponentials as a function of depth makes it possible to establish inventories for each site (Table 4) as well as average inventories (Fig. 6). The percentage of the extrapolated density activities does not exceed 2% for ^{137}Cs and ^{238}Pu and 5% for $^{239+240}\text{Pu}$ of the total inventory for each site beyond approximately 45 g.cm^{-2} depth, while for ^{240}Pu and ^{239}Pu , deduced from ICPMS measurements, and ^{241}Am measured only up to about 27 g.cm^{-2} , it can reach up to about 25%. For average inventories, this share of the extrapolated activity is less

than 12%. Whatever the proportions of deposits in 1963 (GF) and 1967 (LF), compared with the past 50 years, the vertical migration velocities remain between 0.2 and 0.3 g.cm⁻².yr⁻¹. These values are similar to those previously measured for Hiva Oa (Bouisset et al., 2018) and other regions of the globe (Bunzl et al., 1995; Komoza, 1999; Orzel and Komoza, 2014). As a result, radionuclides migrate slowly and half of inventories remain at depths of less than 10 g.cm⁻², except for Ga7 where the values are slightly higher (from 10.3 to 13.0 g.cm⁻².yr⁻¹ depending on the radionuclides). The vertical migration velocities of ²³⁹⁺²⁴⁰Pu and ¹³⁷Cs are not identical; they differ up to 35% depending on the site (Table 4). ¹³⁷Cs/²³⁹⁺²⁴⁰Pu migration velocity ratios for Ga2, Ga5 and Ga6 are higher, 1.15-1.29, than those of Ga1, Ga3 and Ga7 at 0.90-0.96. Approximately the same values are found for the median depth ratios of ¹³⁷Cs and ²³⁹⁺²⁴⁰Pu inventories for all sites (Table 4). This variation may be related to different migration kinetics of caesium and plutonium according to the soil composition, but also because LF and GF, having different ¹³⁷Cs/²³⁹⁺²⁴⁰Pu ratios, were not deposit in the same proportion on each site. This feature is not taken into account in the calculation of migration velocities and this is probably the main reason for this apparent difference. Moreover, the ¹³⁷Cs/²³⁹⁺²⁴⁰Pu inventory ratios are lower for Ga2, Ga5 and Ga6, 3.6-3.9, while they are higher for Ga1, Ga3 and Ga7, 4.4-7.2, indicating fallout with different activity ratios over time (i.e. GF and LF).

Table 4

Inventories, percentage of the extrapolated activity densities, ¹³⁷Cs/²³⁹⁺²⁴⁰Pu vertical migration velocity and median ratios.

Site	Inventory (Bq.m ⁻²) (% extrapolated)						Vertical migration velocity ratio ¹³⁷ Cs/ ²³⁹⁺²⁴⁰ Pu	Median ratio
	¹³⁷ Cs	²³⁹⁺²⁴⁰ Pu	²³⁹ Pu	²⁴⁰ Pu	²⁴¹ Am	²³⁸ Pu		
Ga1	481 ± 32 (0.1)	108.6 ± 5.3 (0.2)	96 ± 11 (1.6)	13.5 ± 1.6 (1.6)	9.82 ± 0.83 (0.5)	5.73 ± 0.77 (1.1)	0.90	0.81
Ga2	573 ± 39 (0.8)	158.2 ± 7.3 (0.3)	156 ± 17 (14)	19.7 ± 2.2 (17)	13.5 ± 1.2 (18)	9.00 ± 1.1 (1.1)	1.17	1.17
Ga3	405 ± 29 (1.4)	80.2 ± 4.2 (1.1)	73.9 ± 7.3 (10)	11.0 ± 1.7 (10)	9.7 ± 1.1 (16)	6.00 ± 0.78 (1.5)	0.96	1.03
Ga5	499 ± 34 (2)	127.0 ± 6.8 (2)	105 ± 12 (3)	16.2 ± 2.3 (5)	13.3 ± 1.5 (6)	7.62 ± 0.86 (0.6)	1.15	1.21
Ga6	433 ± 30 (0.5)	118.7 ± 6.4 (0.1)	109 ± 12 (1.1)	12.1 ± 1.4 (6)	8.8 ± 1.3 (19)	6.49 ± 0.83 (0.1)	1.29	1.29
Ga7	607 ± 42 (1.5)	84.8 ± 5.2 (3)	76.7 ± 7.0 (19)	15.6 ± 1.6 (21)	13.9 ± 1.5 (22)	6.03 ± 1.0 (1.7)	0.95	1.00
Average Ga1-Ga7	499 ± 34 (1.0)	113.0 ± 5.9 (1.0)	106 ± 11 (11)	14.7 ± 1.7 (11)	11.3 ± 1.2 (12)	6.82 ± 0.87 (1.1)	1.09	1.11

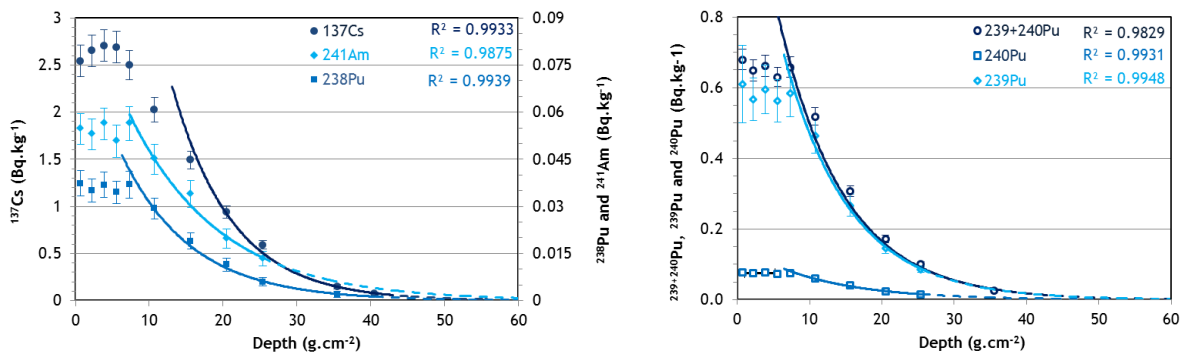


Fig. 6. Average activity concentrations vs depth and exponential extrapolation beyond measured layers (dotted curves).

4.3.1 ^{137}Cs inventory

The ^{137}Cs inventories over the six sites in Gambier are in the range $405\text{--}607\text{ Bq.m}^{-2}$ with an average value of $499 \pm 34\text{ Bq.m}^{-2}$ (Table 4). These values are much higher than those resulting from GF at $20\text{--}30^\circ\text{S}$ estimated about 300 Bq.m^{-2} (UNSCEAR, 2000) and that the inventory in Hiva Oa (10°S), $227 \pm 11\text{ Bq.m}^{-2}$, the latter being in good agreement with GF in the corresponding latitude band. In the same latitude range than Gambier, extreme values up to $1,000\text{ Bq.m}^{-2}$, with a wide range of variation between remote sites, were reported in Chile (Schuller et al., 2002) and in Brazil (Handl et al., 2008), decay corrected to 2018.

4.3.2 $^{239+240}\text{Pu}$, ^{239}Pu and ^{240}Pu inventories

The $^{239+240}\text{Pu}$ inventories over the six sites in Gambier are in the range $80\text{--}158\text{ Bq.m}^{-2}$ with an average value of $113.0 \pm 5.9\text{ Bq.m}^{-2}$ (Table 4), much higher value than 12.3 Bq.m^{-2} for GF ($20\text{--}30^\circ\text{S}$) considering that plutonium follows the same latitudinal distribution as ^{90}Sr (Thakur et al., 2017). The $^{239+240}\text{Pu}$ inventory at Hiva Oa, $12.1 \pm 1.5\text{ Bq.m}^{-2}$, higher than that of 7.8 of GF at $0\text{--}20^\circ\text{S}$, is ten times lower than the one in Gambier. The $^{239+240}\text{Pu}$ contribution to the LF in Gambier is estimated between 84% and 93%. Such values of inventories in Gambier have not been observed in the Southern Hemisphere. The highest values, $71 \pm 2\text{ Bq.m}^{-2}$, have been reported at La Parva (33°S , Chile) (Chamizo et al., 2011) and $51.8 \pm 1.02\text{ Bq.m}^{-2}$ for a soil sample (id. T-03) in Madagascar ($18\text{--}19^\circ\text{S}$) (Rääf et al., 2017). These high inventories in the Gambier are due to the high but uneven contributions of the both isotopes, ^{239}Pu and ^{240}Pu , whose respective average inventories are $106 \pm 11\text{ Bq.m}^{-2}$ and $14.7 \pm 1.7\text{ Bq.m}^{-2}$. The ^{239}Pu inventory is nearly fifteen times higher than that of the average GF fallout of 7.3 Bq.m^{-2} while the ^{240}Pu inventory is only three times higher than that of the average GF of 4.9 Bq.m^{-2} at $20\text{--}30^\circ\text{S}$ (UNSCEAR, 2000).

4.3.3 ^{238}Pu inventory

A third large source term of ^{238}Pu (SNAP) generated a deposit about seven times larger than that of GF in the Southern Hemisphere. However, we can estimate that three quarters of the ^{238}Pu in the Gambier come from the LF. The ^{238}Pu inventories in Gambier range $5.7\text{--}9.0\text{ Bq.m}^{-2}$ with an average value of $6.82 \pm 0.87\text{ Bq.m}^{-2}$ (Table 4). It is nearly five times higher than the $1.21 \pm 0.45\text{ Bq.m}^{-2}$ of Hiva Oa, a value similar to $1.56 \pm 0.60\text{ Bq.m}^{-2}$ obtained in Raivavae (Bouisset et al., 2018), located at the same latitude as the Gambier and test sites. The value at Raivavae is comparable to the average value of $2.1 \pm 1.2\text{ Bq.m}^{-2}$ ($n = 7$) of the inventory made between October 1970 and January

1971 at 20-30°S (Hardy et al., 1973). The highest values, 3.0 and 4.4 Bq.m⁻², included in Hardy's inventory, were measured for two sites in Brazil at the same latitude (23°S) as Gambier.

4.3.4 ²⁴¹Am - ²⁴¹Pu inventory

The ²⁴¹Am inventories over the six sites range 8.8-13.9 Bq.m⁻² with an average value of 11.3 ± 1.2 Bq.m⁻² (Table 4), i.e. more than twice the cumulative GF value of 4.6 Bq.m² calculated from the annual decrease of ²⁴¹Pu at 20-30°S. The only comparative data we have in French Polynesia are those of the 4-6 cm section at Hiva Oa in 2016 (Table 3) with concentrations varying from 0.0195 ± 0.0061 Bq.kg⁻¹ to 0.0435 ± 0.0074 Bq.kg⁻¹. For the six Gambier sites, at the same depth, concentrations are about twice higher, between 0.00392 ± 0.0040 Bq.kg⁻¹ to 0.0892 ± 0.0075 Bq.kg⁻¹. The average ²⁴¹Pu inventory calculated from ²⁴¹Am applying Eq. (5) is 33.7 ± 3.4 Bq.m⁻² in Gambier, with an initial deposit in 1967 and decay corrected to 2018. The residual activity of ²⁴¹Pu from GF in 2018, calculated from the annual fallout, is estimated to be 10.8 Bq.m⁻² and 6.9 Bq.m⁻² at 0-20°S and 20-30°S respectively. The ²⁴¹Pu inventory in the Gambier is thus estimated to be three times higher than that of the average GF deposition at 20-30°S. The variability of inventories from one site to another is related to precipitation frequencies and intensities. In particular, LF deposition is dependent on the probability of a rainy event over a few hours while GF has deposited on the multi-year scale. Our assessments of LF and GF contributions from inventories were based on a latitudinal average of GF. A more precise distribution of the contribution of the two fallout sources can be obtained from the mixing equations, as we will see later.

Table 5

Activity and atom ratios (26) in Gambier and Hiva Oa. Signatures of LF, French test sites and GF are detailed in the text. Data are decay corrected to 2018.

	Hiva Oa	Gambier	LF	Moruroa	Fangataufa	GF
Sampling date	2016	2018	-	1996	1996	-
Activity ratio ± 2σ (Bq/Bq)						
¹³⁷ Cs/ ²³⁹⁺²⁴⁰ Pu	18.7 ± 3.1 ^a	4.42 ± 0.37	2.0 ± 0.4	0.08 ± 0.03 ^b	0.51 ± 0.06 ^b	24.4 ^d
²³⁸ Pu/ ²³⁹⁺²⁴⁰ Pu	0.10 ± 0.05 ^a	0.060 ± 0.008	0.045 ± 0.008	0.0052 ± 0.0026 ^b	0.325 ± 0.039 ^b	0.12 ± 0.04 ^e
²⁴¹ Am/ ²³⁹⁺²⁴⁰ Pu	0.37 ± 0.08 [*]	0.100 ± 0.011	0.031 0.009	0.025 ± 0.008 ^b	0.070 ± 0.012 ^b	0.38 ^d
²⁴¹ Pu/ ²³⁹⁺²⁴⁰ Pu	0.90 ± 0.20 [*]	0.298 ± 0.034	0.092 ± 0.027	0.074 ± 0.022	0.209 ± 0.037	0.98 ^d
Eq. (5)	(t ₀ in 1963)	(t ₀ in 1967)		(t ₀ in 1967)	(t ₀ in 1967)	(annual deposition)
Atom ratio ± 2σ (at./at.)						
(²⁴⁰ Pu/ ²³⁹ Pu) _{AR}	0.142 ± 0.012	0.040 ± 0.004	0.0176 ± 0.0049	0.018 ± 0.005 ^c	0.049 ± 0.001 ^c	0.182 ^d 0.173 ± 0.027 ^f
(²⁴¹ Pu/ ²³⁹ Pu) _{AR}	(8.2 ± 1.9)10 ⁻⁴	(2.03 ± 0.31)10 ⁻⁴	(0.55 ± 0.23)10 ⁻⁴	(0.47 ± 0.20)10 ⁻⁴	(1.47 ± 0.26)10 ⁻⁴	9.7 10 ⁻⁴ ^d (7.25 ± 2.52)10 ⁻⁴ ^f
Eq. (6)						

^{*} From sections (4-6 cm) of four sites.

^a (Bouisset et al., 2018), ^b(IAEA, 1998), ^c(Hrnecek et al., 2005), ^d(UNSCEAR, 2000).

^e In Southern Hemisphere, including SNAP-9A and NWTs fallout (Hardy et al., 1973).

^f Soil collected in 1970-1971 in the 0-30°S latitude range (Kelley et al., 1999).

4.4 Activity and atom ratios

4.4.1 $^{238}\text{Pu}/^{239+240}\text{Pu}$ activity ratios

The average $^{238}\text{Pu}/^{239+240}\text{Pu}$ activity ratio measured in the Gambier is 0.060 ± 0.008 , ranging from 0.053 to 0.075 for all six sites. These activity ratios are globally in the range of those observed at this latitude, 0.071 ± 0.033 in the soils of Raivavae (Bouisset et al., 2018) or 0.08 ± 0.01 in the oceanic water column (station Hy12, 20°S - 101°W) (Kishonita et al., 2011). For the highest activities in soils of Gambier, therefore concerning the first soil sections, $^{238}\text{Pu}/^{239+240}\text{Pu}$ activity ratios decrease as shown in Fig. 7-a. The $^{238}\text{Pu}/^{239+240}\text{Pu}$ inventory ratios also decrease when $^{239+240}\text{Pu}$ inventories increase to about $100 \text{ Bq}\cdot\text{m}^{-2}$ (Fig. 7-b). Beyond this value, $^{238}\text{Pu}/^{239+240}\text{Pu}$ activity ratios, much less influenced by the fallout of SNAP, stabilize at an average value for four of the six sites at 0.056 ± 0.007 . This ratio is therefore almost exclusively related to the mixture of Fangataufa fallout ($^{238}\text{Pu}/^{239+240}\text{Pu}$ ratio of 0.325), about 15%, and Moruroa fallout (ratio of 0.0052), about 85%

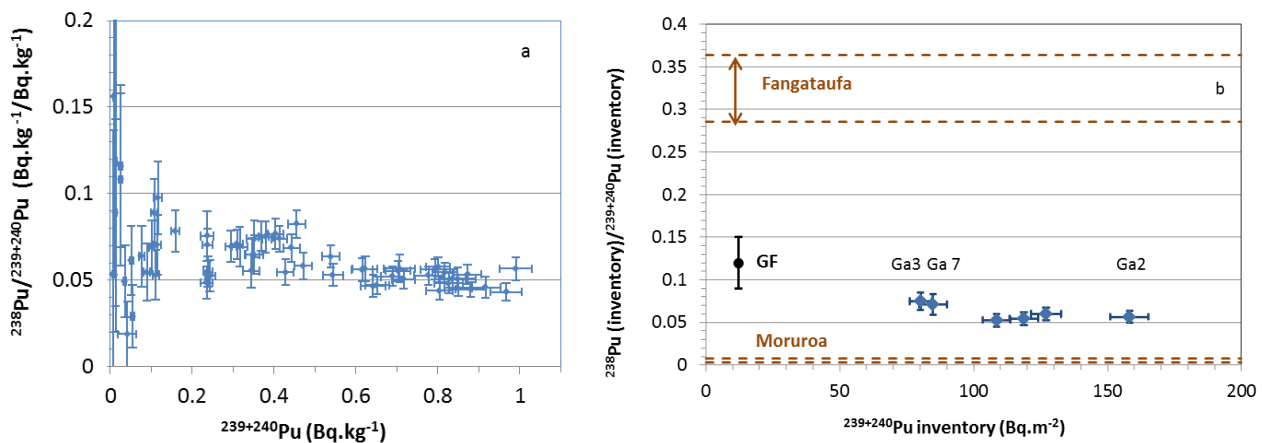


Fig. 7. a- $^{238}\text{Pu}/^{239+240}\text{Pu}$ vs $^{239+240}\text{Pu}$ in all samples of Gambier. b- Inventory ratios of $^{238}\text{Pu}/^{239+240}\text{Pu}$ vs $^{239+240}\text{Pu}$ inventories for the six sites. Dashed lines indicate $^{238}\text{Pu}/^{239+240}\text{Pu}$ activity ratios of both test sites. GF is $^{238}\text{Pu}/^{239+240}\text{Pu}$ (Hardy et al., 1973) at 20 - 30°S .

4.4.2 $^{241}\text{Am}/^{239+240}\text{Pu}$ and $^{241}\text{Pu}/^{239+240}\text{Pu}$ activity ratios

The average $^{241}\text{Am}/^{239+240}\text{Pu}$ activity ratio in the Gambier is 0.100 ± 0.011 . The value is significantly higher, 0.37 ± 0.08 , for 4-6 cm sections of the four Hiva Oa sites, which is consistent with the 0.38 value assigned to GF. For these same sections of the six Gambier sites, the average values are 0.093 ± 0.034 , close to the average value given above for the entire inventory. The calculated $^{241}\text{Pu}/^{239+240}\text{Pu}$ activity ratio, assuming that all the inventory comes from the LF deposited in 1967, is 0.298 ± 0.034 in the Gambier. This ratio is three times higher than that calculated for the sections of the four Hiva Oa sites, 0.90 ± 0.20 , this being compatible with the one to 0.96 for GF. For the highest concentrations in $^{239+240}\text{Pu}$ in the Gambier, the $^{241}\text{Pu}/^{239+240}\text{Pu}$ activity ratios are close to 0.1 (Fig. 8). The decrease in this ratio is of the order of a factor of five between the deepest layers and the surface while the $^{240}\text{Pu}/^{239+240}\text{Pu}$ decreases only by a factor two and the $^{239}\text{Pu}/^{239+240}\text{Pu}$ increases by about 10%. These variations reflect the fallout of high-yield explosions from the Northern Hemisphere (in depth) and those from LF due to low-yield explosions (at ground surface) that generate few neutrons. The low generation rate of ^{240}Pu and ^{241}Pu by neutron capture is consistent with the low fission rate ($^{137}\text{Cs}/^{239+240}\text{Pu}$ low) from LF.

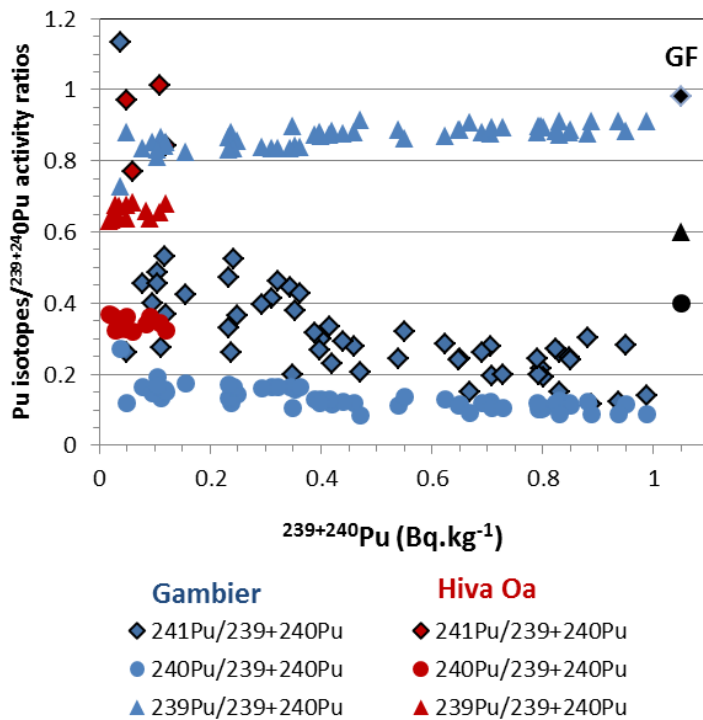


Fig. 8. ²⁴¹Pu, ²⁴⁰Pu, ²³⁹Pu /²³⁹⁺²⁴⁰Pu activity ratios vs ²³⁹⁺²⁴⁰Pu activity concentration. Symbols in black are related to GF ratios from global inventory (UNSCEAR, 2000).

4.4.3 ¹³⁷Cs/²³⁹⁺²⁴⁰Pu activity ratios

For all the sections measured for the six sites in the Gambier, and for comparison those of the four sites in Hiva Oa (Bouisset et al., 1998), the concentration of ²³⁹⁺²⁴⁰Pu increase with the concentration of ¹³⁷Cs (Fig. 9). The average ¹³⁷Cs/²³⁹⁺²⁴⁰Pu ratio of inventories is 4.42 ± 0.37 , much lower than that of 13.6 ± 2.7 measured at the same latitude at Raivavae (Bouisset et al., 2018). Although ¹³⁷Cs and ²³⁸Pu concentrations at Ga3 and Ga7 sites are very different from those at Ga1, all three sites are more influenced by GF than the other three sites. The higher inventory for Ga1 (Aukena island) must be related to a different precipitation regime although this island is not far (a few kilometers) from the other islands. The contribution to GF, slightly older than that to LF, is higher in the deepest layers of the six sites. This observation is also valid for Hiva Oa, where the values in the deepest layers are close to those of the GF, with a ratio ¹³⁷Cs/²³⁹⁺²⁴⁰Pu close to 21 while it reduces to 0.16 at ground surface. ¹³⁷Cs/²³⁹⁺²⁴⁰Pu at Hiva Oa, 18.7 ± 3.1 (Table 5), is lower than the GF ratio at 24.4. There is little comparative data in the Southern Hemisphere. Widely dispersed values, 33.7 ± 11.3 (10-50) were measured in Australia on soils in the Sydney Basin (Smith et al., 2016). ¹³⁷Cs/²³⁹⁺²⁴⁰Pu close to 7, similar to those of the Gambier, was observed in depth at Searchlight (150 km from the NTS). In this place, the ¹³⁷Cs/²³⁹⁺²⁴⁰Pu ratios are increasing to values of 15-16 going up to the surface because the average global fallout is, unlike the Gambier, posterior to the LF. A similar ratio was also measured in depth at the Queen City Summit site (55 km from NTS) but with decreasing values, up to 0.4-0.5 when rising towards the surface, following recent wind inputs from NTS (Turner et al., 2003). Excess of inventories in ¹³⁷Cs and ²³⁹⁺²⁴⁰Pu in Gambier gives a ¹³⁷Cs/²³⁹⁺²⁴⁰Pu of 2.0 ± 0.4 for LF, much higher than that of the ratios on the Fangataufa (0.51) and Moruroa (0.08) sites. The signatures in ¹³⁷Cs/²³⁹⁺²⁴⁰Pu on the test sites deduced from the

measurements taken on the samples taken in 1996 (IAEA, 1999), are therefore not those of the LF in the Gambier.

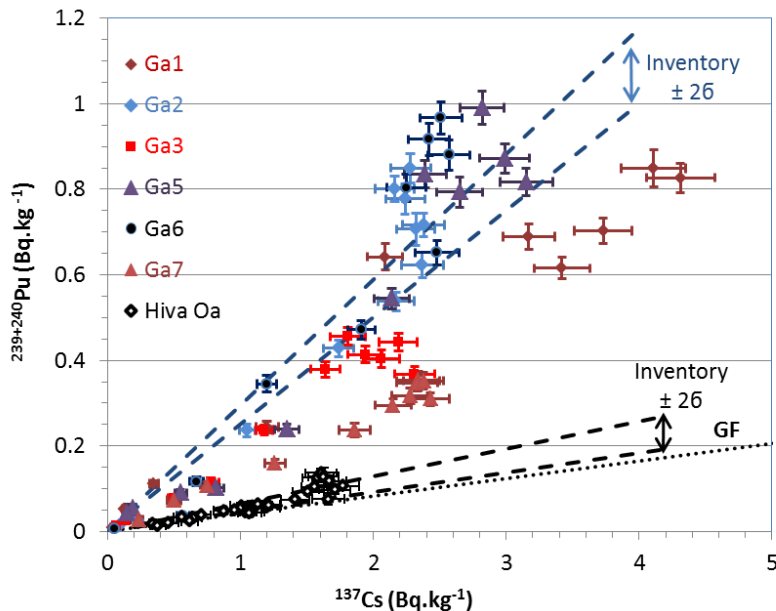


Fig. 9. $^{239+240}\text{Pu}$ vs ^{137}Cs in Gambier (this work) and Hiva Oa (Bouisset et al., 2018). Dotted lines are the average ratios from inventory at Gambier, Hiva Oa and GF.

4.4.4 $(^{240}\text{Pu}/^{239}\text{Pu})_{\text{AR}}$

$(^{240}\text{Pu}/^{239}\text{Pu})_{\text{AR}}$ is higher in the deepest layers due to the older contribution of GF (Fig. 10). When activities in $^{239+240}\text{Pu}$ increase, the $(^{240}\text{Pu}/^{239}\text{Pu})_{\text{AR}}$ tend towards the value assigned to Moruroa, more particularly for Ga2 and Ga6. Both sites are characterized by $^{137}\text{Cs}/^{239+240}\text{Pu}$ of 3.6, lower than other sites (3.9-7.2), showing that the contribution of LF to inventories is higher than at other sites. The average ratio $(^{240}\text{Pu}/^{239}\text{Pu})_{\text{AR}}$ for the six sites is 0.040 ± 0.004 , ranging from 0.032 (Ga6) to 0.54 (Ga7). This ratio was calculated on the basis of the values of all the measured sections, i.e. for a depth of about 27 g.cm^{-2} , weighted by the activity density $^{239+240}\text{Pu}$ of each section. The proportion of extrapolated inventory represents less than 2% for the Ga1 and Ga6 sites, up to nearly 12% for the Ga7 site. This fraction of the inventory was taken into account assuming that the ratio $(^{240}\text{Pu}/^{239}\text{Pu})_{\text{AR}}$ of the last measured section is unchanged at higher depths, leading to a higher ratio $(^{240}\text{Pu}/^{239}\text{Pu})_{\text{AR}}$ of up to 3% for the Ga6 site. These atom ratios are much lower than those measured at Hiva Oa where the average value for sections 4-6 cm, 6-8 cm and 10-15 cm is 0.142 ± 0.012 . Similar values were obtained for the whole Australian continent, with the lowest values in regions affected by LF of the English tests (Tims et al., 2013), in Cook Islands (Froehlich et al., 2019) at the same latitude than Gambier Islands and in South America (Peru, Argentina, Chile), between 12°S and 42°S , sampled in 1970-1971 (Kelley et al., 1999). The ratios were averaged a little lower at $0-30^\circ\text{S}$ with soils sampled between October 1970 and January 1971. These values, as well as more recent data for the Southern Hemisphere, are grouped together in Fig. 11. Signatures for test sites in Australia and French Polynesia are also shown in this figure. Local effects of test sites are clearly observed at near latitudes and/or relatively short distances from test sites with the exception for the Parva result (Chamizo et al., 2011), which may be the result of direct tropospheric French-test debris. This is also the case of the two values measured in Brazil for samples collected by the EML

(Kelley et al., 1999). In the 10°-35°S latitude range, the values for EML samples collected in the early 1970s are generally higher than those collected later. The tropospheric and stratospheric fallout of the French tests after 1970 are not fully taken into account in these EML samples.

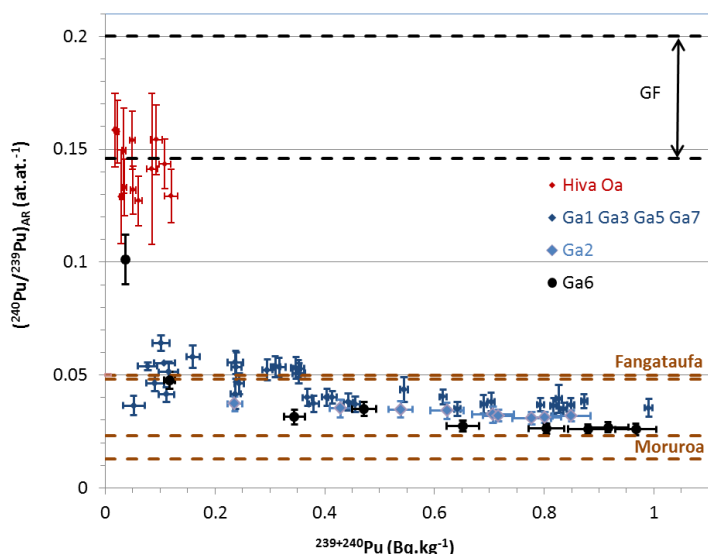


Fig. 10. $(^{240}\text{Pu}/^{239}\text{Pu})_{\text{AR}}$ vs $^{239+240}\text{Pu}$ activity concentrations in Gambier and Hiva Oa soils (all layers measured). Dotted lines are GF values at 0-30°S (Kelley et al., 1999) and for Moruroa and Fangataufa (Hrneck et al., 2005).

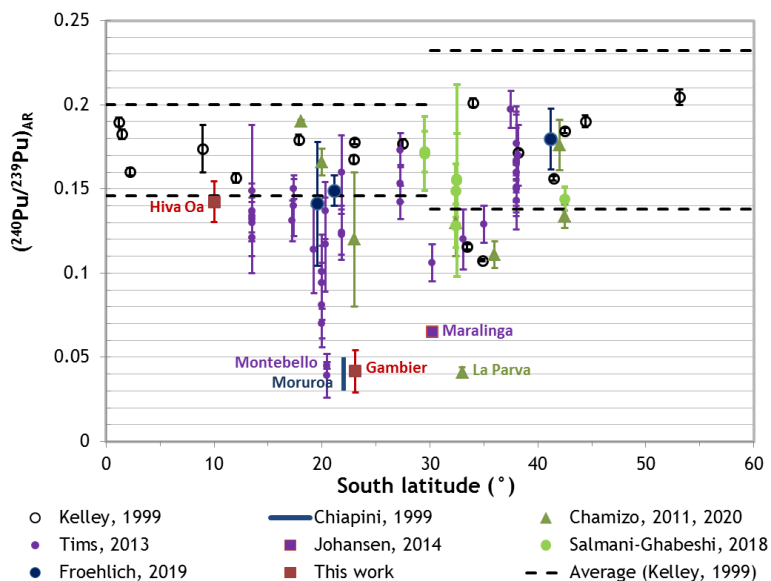


Fig. 11. $(^{240}\text{Pu}/^{239}\text{Pu})_{\text{AR}}$ vs southern latitude.

The stratospheric injection of French-test debris was observed with the measurement of air filters collected by the Health and Safety laboratory, from 1963 to 1970, at 40°S and 12-20 km above sea level above the tropopause (Hardy, 1973). $(^{240}\text{Pu}/^{239}\text{Pu})_{\text{AR}}$, 0.181 ± 0.005 (Table 6), measured during 1963 to 1966 are close to those of GF from Northern Hemisphere. Average ratio decrease at 0.168 ± 0.011 in 1967-1968, for filters collected after the 1967 test campaign and before these of 1968. This reduction of $(^{240}\text{Pu}/^{239}\text{Pu})_{\text{AR}}$ compared to previous years is therefore mainly due to the tests conducted during 1966-1967 (eight tests for a cumulated yield of 0.68 Mt).

Average ratio of 0.111 ± 0.021 was measured in February 1969 and January 1970 following the 1968 campaign (five tests for a cumulated yield of 4.6 Mt) and before the one of 1970 (no campaign in 1969). The evolution of these ratios is clearly associated with the stratospheric injection of the Moruroa and Fangataufa tests combined with residual fallout from the high-yield US and USSR tests of 1961-1962 (83 Mt) and those of the three Chinese tests of 3 Mt each in 1967, 1968 and 1970, and for which about 25% of stratospheric radioactive debris was transferred to the stratosphere of the Southern Hemisphere. $(^{240}\text{Pu}/^{239}\text{Pu})_{\text{AR}}$ in the Northern Hemisphere between 1966 and 1977, Chinese tests in particular, were measured on grass samples from the Rothamsted archives, Harpenden UK (Warneke et al., 2002). Except the ratio of 0.169 in 1972, all other ratios are greater than 0.2 (0.202-0.262). High $^{240}\text{Pu}/^{239}\text{Pu}$ ratios 0.172 to 0.22 (Dong et al, 2010), 0.194 ± 0.004 (Huang et al., 2019), have been recently measured in the central China. Measurements in soils collected between October 1970 and January 1971 in 0° - 30°S latitude range indicate lower ratios than those in the Northern Hemisphere (Kelley et al., 1999). These results take into account a little more than 50% of the tropospheric and stratospheric French-test debris, the other half of the fallout being after the period of collection of these samples. The $(^{240}\text{Pu}/^{239}\text{Pu})_{\text{AR}}$ measured at 37 sites across Australia clearly show an impact of the local UK-test debris in the centre of the continent (Tims et al., 2013). The average ratios are 0.156 for sites in the east, not affected by local fallout. For 14 sites in the Sydney Basin, the values are more dispersed with an average of 0.146 ± 0.013 (Smith et al., 2016). For sampling at Brisbane at the beginning of 1970, the measured value was 0.177 ± 0.003 (Kelley et al., 1999), while that of the sampling of the years 2010 is 0.156 ± 0.010 (Tims et al., 2013). There are also differences between the $^{137}\text{Cs}/^{239+240}\text{Pu}$ activity ratio of GF, 24.4, and that measured at 21.1 ± 1.2 in north-eastern Queensland, Australia. This low activity ratio is associated with a low $(^{240}\text{Pu}/^{239}\text{Pu})_{\text{AR}}$ of 0.149 ± 0.003 (Everett et al., 2008), lower than the 0.173 assigned to GF in the 0 - 30°S latitude range (Kelley et al., 1999). These results in Australia are close to those measured at Hiva Oa $(^{240}\text{Pu}/^{239}\text{Pu})_{\text{AR}} = 0.142 \pm 0.012$ et $^{137}\text{Cs}/^{239+240}\text{Pu} = 18.7 \pm 3.1$, which is weakly impacted by the local fallout of the French tests and perhaps a little by the low-yield tests of Christmas Island. The stratospheric and tropospheric deposition of the French tests after the 1970s were partly or totally responsible for the $^{137}\text{Cs}/^{239+240}\text{Pu}$, $(^{240}\text{Pu}/^{239}\text{Pu})_{\text{AR}}$ and $(^{241}\text{Pu}/^{239}\text{Pu})_{\text{AR}}$ ratios lower than those assessed for the Northern Hemisphere, or those resulting from the measurement of samples collected in the early 1970s.

Table 6

Atom ratios (16, at the date of collection) in air filtered samples collected from 12 to 21 km at 40°S (Hardy, 1973).

Location	Date of collection	Number of values	Atom ratio		Activity ratio ¹
			$(^{240}\text{Pu}/^{239}\text{Pu})_{\text{AR}}$	$(^{241}\text{Pu}/^{239}\text{Pu})_{\text{AR}}$	$^{241}\text{Pu}/^{239+240}\text{Pu}$
40°S-145°W (1963-1965) 40°S-70°W (1966)	27 Aug 1963 - 3 Jul 1966	25	0.181 ± 0.005	0.012 ± 0.002	12.2 ± 1.5
40°S-70°W	9 Jan 1967 - 16 Jun 1968	26	0.168 ± 0.011	0.011 ± 0.003	11.3 ± 2.7
	3 Feb 1969 - 19 Jan 1970	14	0.111 ± 0.021	0.006 ± 0.002	7.4 ± 2.4

¹ calculated applying Eq.6.

4.4.5 $(^{241}\text{Pu}/^{239}\text{Pu})_{\text{AR}}$

Fig. 12. shows the $(^{241}\text{Pu}/^{239}\text{Pu})_{\text{AR}}$, calculated from $^{241}\text{Pu}/^{239+240}\text{Pu}$ activity ratios and $(^{240}\text{Pu}/^{239}\text{Pu})_{\text{AR}}$ with Eq. (6), for sections 0-30 cm of the six sites of the Gambier and section 4-6 cm of the four Hiva Oa sites, according to $^{239+240}\text{Pu}$ activity concentration. As for the $(^{240}\text{Pu}/^{239}\text{Pu})_{\text{AR}}$ (Fig. 10), the $(^{241}\text{Pu}/^{239}\text{Pu})_{\text{AR}}$ in the first sections of Ga3 are higher, less influenced by Moruroa fallout, than they are in the equivalent sections of other sites. For shallow soil layers at all sites, the $(^{241}\text{Pu}/^{239}\text{Pu})_{\text{AR}}$ are more influenced by recent LF while those at depth have a somewhat higher relative contribution from the GF. For all sections, the values in Gambier are lower than those in GF (Fig. 12) while those in Hiva Oa are compatible. Average $(^{241}\text{Pu}/^{239}\text{Pu})_{\text{AR}}$ at Gambier is $(2.03 \pm 0.31)10^{-4}$, three times lower than that at $6.1 \cdot 10^{-4}$ measured in the stratosphere in 1969-1970, decay corrected to 2018. The ratio in the stratosphere before 1966, $9.3 \cdot 10^{-4}$, is close to the mean value $(8.2 \pm 1.9)10^{-4}$ of Hiva Oa.

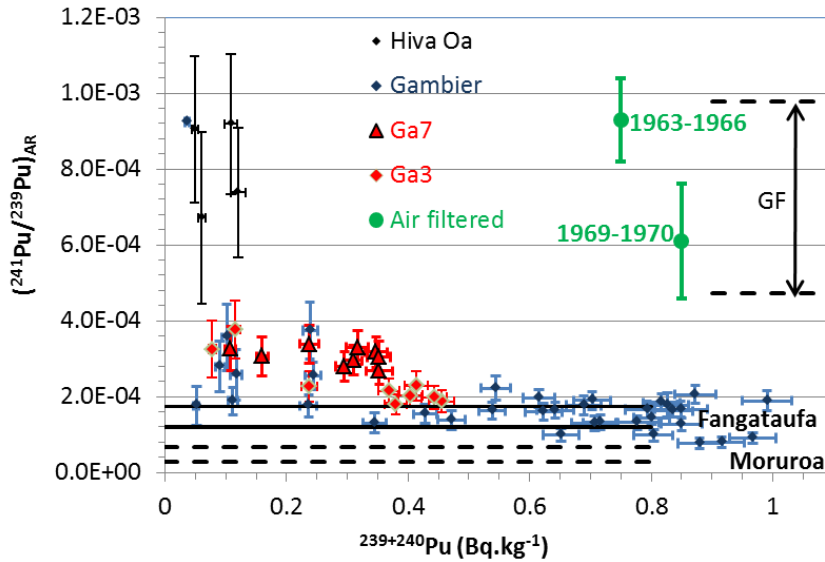


Fig. 12. $(^{241}\text{Pu}/^{239}\text{Pu})_{\text{AR}}$ vs $^{239+240}\text{Pu}$ activity concentrations in Gambier and Hiva Oa (all soil layers measured). Dotted lines are GF values at 0-30°S (Kelley et al., 1999) and LF from signatures of Moruroa and Fangataufa. The $(^{241}\text{Pu}/^{239}\text{Pu})_{\text{AR}}$ for stratospheric air filtered before French tests period (1963-1966) and during tests period (1969-1970) are also reported (Hardy, 1973).

4.5 LF and GF proportions deduced from a two member mixing model

4.5.1 $^{241}\text{Am}/^{239+240}\text{Pu}$ - $^{238}\text{Pu}/^{239+240}\text{Pu}$ mixing lines

The mixing line ML from Eq. (2) is defined by the inventory ratio $^{241}\text{Am}/^{239+240}\text{Pu}$ vs $^{238}\text{Pu}/^{239+240}\text{Pu}$ in Gambier and for GF (Fig. 13). The mean values of the activity ratios of the four sections (4-6 cm) of Hiva Oa are compatible with those of the GF. LF ratios, in the extension of the ML line, are bounded by the y-axis, $^{241}\text{Am}/^{239+240}\text{Pu} = 0$, and the lowest ratios measured in the first sections of the Ga6 site, 0.04. The LF point is at the intersection of the two mixing lines ML and MLT. The signatures of the LF in the Gambier from Eq. (4) are $^{241}\text{Am}/^{239+240}\text{Pu} = 0.031 \pm 0.009$ and $^{238}\text{Pu}/^{239+240}\text{Pu} = 0.045 \pm 0.008$. The proportion of Moruroa fallout in LF, applying Eq. (1), is 87% (13% for Fangataufa). LF accounts for an average of 80% of fallout to the Gambier and GF 20%. Applying Eq. (6), with $t_1=t_2$ and $t_0 = 51$ yr. (1967), the $^{241}\text{Pu}/^{239+240}\text{Pu}$ ratio of LF in 2018 is 0.092 ± 0.027 .

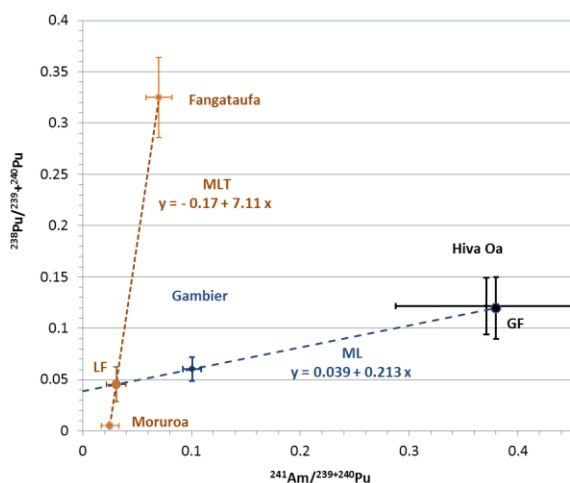


Fig. 13. $^{238}\text{Pu}/^{239+240}\text{Pu}$ - $^{241}\text{Am}/^{238+239}\text{Pu}$ mixing lines (ML) between Gambier inventories and GF. The values of Hiva Oa are averages of the four sections (4-6 cm) measured. The brown dotted line is the MLT mixing line of fallout from Moruroa and Fangataufa. The LF point corresponds to the intersection of the ML and MLT mixing lines, i.e. the signature of the mixing of the fallout from both test sites.

4.5.2 $(^{241}\text{Pu}/^{239}\text{Pu})_{\text{AR}}$ - $(^{240}\text{Pu}/^{239}\text{Pu})_{\text{AR}}$ mixing lines

$(^{241}\text{Pu}/^{239}\text{Pu})_{\text{AR}}$ vs $(^{240}\text{Pu}/^{239}\text{Pu})_{\text{AR}}$ for the six sites in Gambier and for the four 4-6 cm layers at Hiva Oa are in the same alignment (Fig. 14). This figure shows the values of GF derived from UNSCEAR (2000) data and those derived from EML sample measurements in the 0-30°S latitude range (Kelley et al, 1999). These data are complemented by the results obtained in the air filters collected in the lower stratosphere at 40°S (Hardy, 1973) and the values of the signatures of the Moruroa and Fangataufa sites. The linear regression line of the air filter values differs slightly from the mixing line between the Gambier mean value and the GF, indicating that the signatures of the LF are almost the same as those of the stratospheric injections of the Moruroa and Fangataufa tests. The signatures measured at the Fangataufa site are not those that contributed to the LF on the Gambier. The $(^{240}\text{Pu}/^{239}\text{Pu})_{\text{AR}}$ and $(^{241}\text{Pu}/^{239}\text{Pu})_{\text{AR}}$ are dependent on each other (Eq. (6)), their values are indicated by the red dotted line on Fig. 14. The interception of this line with the MLT line, by imposing the constraint that the contribution to the LF of Fangataufa is of 13% (value established previously), $(^{240}\text{Pu}/^{239}\text{Pu})_{\text{AR}} = 0.0135 \pm 0.0038$ and $(^{241}\text{Pu}/^{239}\text{Pu})_{\text{AR}} = (1.29 \pm 0.53)10^{-4}$, is the signature of the LF from Fangataufa in the Gambier. LF signatures, at the intersection of MLT and ML from Eq. (4), are $(^{240}\text{Pu}/^{239}\text{Pu})_{\text{AR}} = 0.0176 \pm 0.0049$ and $(^{241}\text{Pu}/^{239}\text{Pu})_{\text{AR}} = (5.5 \pm 2.3)10^{-5}$. Although the values of the ratios, at two standard deviation, of the six sites are compatible with the ML mixing line, they are not fully aligned. It is very likely that the radioactive fallout from Fangataufa and Moruroa was not homogeneous over the archipelago due to variable local precipitation.

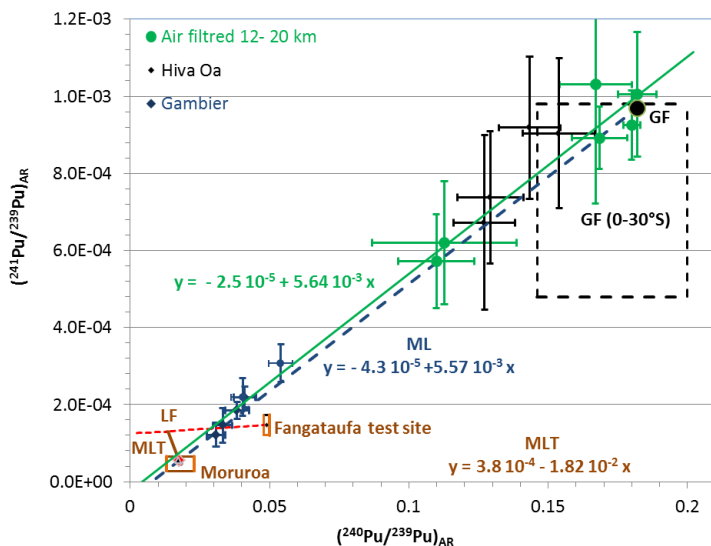


Fig. 14. $(^{241}\text{Pu}/^{239}\text{Pu})_{\text{AR}}$ vs $(^{240}\text{Pu}/^{239}\text{Pu})_{\text{AR}}$ for Gambier, Hiva Oa (this study) Morurooa, Fangataufa derived from data from (Hrnecek et al., 2005), GF (0-30°S) from (Kelley and al., 1999), GF derived from (UNSCEAR, 2000) and air samples measured in the low stratosphere from 1963 to 1970 (Hardy, 1973). The green line is the linear regression for air samples, the black dotted line the GF-Gambier mixing line.

4.5.3 $^{238}\text{Pu}/^{239+240}\text{Pu}$ - $(^{240}\text{Pu}/^{239}\text{Pu})_{\text{AR}}$ mixing lines

The ML mixing line is defined by the Gambier $^{238}\text{Pu}/^{239+240}\text{Pu}$ vs $(^{240}\text{Pu}/^{239}\text{Pu})_{\text{AR}}$ inventory ratios and GF ratios (Fig. 15). The mixing line (black dotted line) linking the signatures of the Morurooa and Fangataufa sites intercepts well the mixing line linking the signatures of the Gambier and those of the GF, at coordinates $(^{238}\text{Pu}/^{239+240}\text{Pu}) = 0.053 \pm 0.005$ et $(^{240}\text{Pu}/^{239}\text{Pu})_{\text{AR}} = 0.023 \pm 0.005$, almost identical to that measured in the first sections of the Ga6 site, 0.026 ± 0.002 (Table 3). With another mixing line, between the signatures of Morurooa and the $(^{240}\text{Pu}/^{239}\text{Pu})_{\text{AR}}$ of the LF of Fangataufa and not to the ratio measured on the atoll, the signature in $(^{240}\text{Pu}/^{239}\text{Pu})_{\text{AR}}$ of the LF is 0.0174, the same as Section 4.4.3. The signature of the LF in $^{238}\text{Pu}/^{239+240}\text{Pu} = 0.053 \pm 0.008$, is a little high but compatible with the value of 0.045 ± 0.008 of Section 4.4.1.

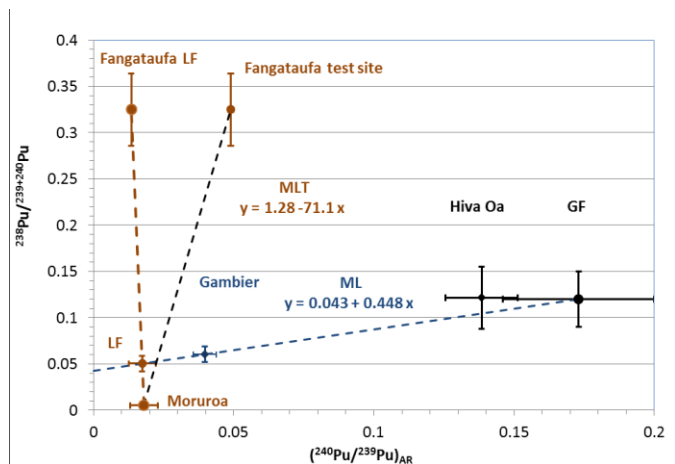


Fig. 15. $^{238}\text{Pu}/^{239+240}\text{Pu}$ - $(^{240}\text{Pu}/^{239}\text{Pu})_{\text{AR}}$ mixing lines (ML) between Gambier inventories and GF. The values of Hiva Oa, mean of the four sections (4-6 cm) measured, and the signatures of both test sites (Table 6) are given.

4.5.4 $^{238}\text{Pu}/^{239+240}\text{Pu}$ - $^{137}\text{Cs}/^{239+240}\text{Pu}$ mixing lines

Alignment of activity ratios of $^{238}\text{Pu}/^{239+240}\text{Pu}$ vs $^{137}\text{Cs}/^{239+240}\text{Pu}$ for Hiva Oa, Raivavae and Gambier confirms that there are only two sources of fallout on these islands (Fig. 16). LF are low in Hiva Oa, higher in Raivavae and important in Gambier. Test site values are indicated with $^{137}\text{Cs}/^{239+240}\text{Pu}$ signatures derived from ^{90}Sr measurements at sites. The ML mixing line is established between the GF and the average ratio of inventories in Gambier. The $^{137}\text{Cs}/^{239+240}\text{Pu}$ ratios of the LF, a continuous brown line on Fig. 16, in the extension of the ML line, are bounded by the lowest $^{137}\text{Cs}/^{239+240}\text{Pu}$ ratio of both test sites (Moruroa) and by the lowest ratios for section 4-6 cm of Ga6 for LF, $^{137}\text{Cs}/^{239+240}\text{Pu}$ activity ratios range 0.08-2.6. The ratio of 2.0 ± 0.4 deduced from the inventories (Section 4.3.3) is acceptable (indicated LF on Fig. 16) as well as the associated activity ratio $^{238}\text{Pu}/^{239+240}\text{Pu}$ of 0.053 ± 0.008 , in the range of that previously determined at 0.045-0.008.

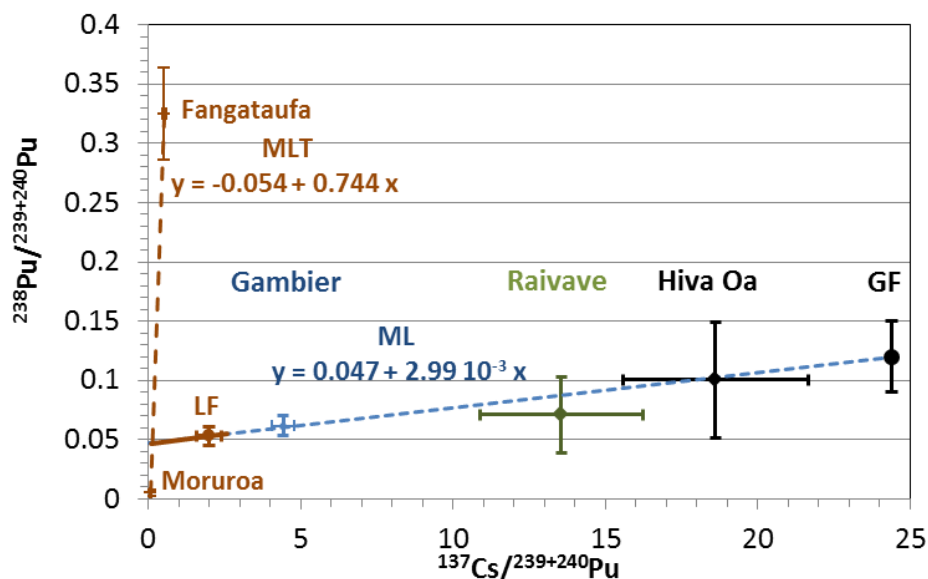


Fig. 16. $^{238}\text{Pu}/^{239+240}\text{Pu}$ - $^{137}\text{Cs}/^{239+240}\text{Pu}$ mixing lines (ML) for Gambier inventories and GF. Results from Raivavae and Hiva Oa are given (Bouisset et al., 2018) as well as the activity ratios measured at both test sites and their MLT mixing line.

4.5.5 Stratospheric fallout signatures in the Southern Hemisphere and proportions of stratospheric and local fallout in Gambier.

The signatures of the stratospheric fallout in the Southern Hemisphere can be evaluated if they are considered to be a combination of those of the Northern Hemisphere and those of the French tests and assuming that the signatures of the LF in the Gambier are close to those of the stratospheric injections from French tests (Fig. 14). The fission energy of the French tests represents 11%, 89% coming from Northern Hemisphere tests, of the injection into the stratosphere of the Southern Hemisphere. The plutonium fraction is higher considering the ratio $^{137}\text{Cs}/^{239+240}\text{Pu}$ specific of the fallout of the French tests established previously, 2.0 ± 0.4 , while that from the tests of the Northern Hemisphere is 24.4. The ratio made up by the combination of both signatures is 21.9 ± 0.1 ($89\% \times 24.4$ and 11% of 2.0). Given the large difference between both contributions, the value calculated for the stratospheric average fallout depends little on the ratio $^{137}\text{Cs}/^{239+240}\text{Pu}$ activity ratio chosen about 2 for the LF. Ratio of 21.9 is compatible with that measured at Hiva Oa 18.7 ± 3.1 , confirming low tropospheric or regional French-test debris on this island. This signature

matches the value of 21.1 ± 1.2 in Queensland, Australia (Everett et al., 2008). With a $^{137}\text{Cs}/^{239+240}\text{Pu}$ ratio of 13.6 ± 2.7 at Raivavae (Fig. 16), the contribution of regional-tropospheric fallout is about 40%. In order to discern the tropospheric share of this fallout in French Polynesia, an inventory of islands in the Société archipelago ($\sim 22^\circ\text{S}$), located more than 1,000 km west of the Moruroa and Fangataufa test sites, is ongoing. From the $^{137}\text{Cs}/^{239+240}\text{Pu}$ ratio and the mixing equations given in Figs. 14 to 17, the other signatures for stratospheric fallout in the Southern Hemisphere are deduced successively (Table 7). $^{241}\text{Pu}/^{239+240}\text{Pu}$ activity ratio is deduced from that of $^{241}\text{Am}/^{239+240}\text{Pu}$ with Eq. (4).

Table 7

Activity ratio and atom ratio signatures for stratospheric fallout in Southern Hemisphere deduced from LF in the Gambier.

Activity ratio	
$^{137}\text{Cs}/^{239+240}\text{Pu}$	21.9 ± 0.1
$^{238}\text{Pu}/^{239+240}\text{Pu}$	0.11 ± 0.05
$^{241}\text{Pu}/^{239+240}\text{Pu}$	1.03 ± 0.12
$^{241}\text{Am}/^{239+240}\text{Pu}$	0.35 ± 0.05
Atom ratio	
$(^{240}\text{Pu}/^{239}\text{Pu})_{\text{AR}}$	0.157 ± 0.011
$(^{241}\text{Pu}/^{239}\text{Pu})_{\text{AR}}$	$(8.28 \pm 0.18) 10^{-4}$

We estimated, from a two-member mixing model with signatures of stratospheric fallout from the Northern Hemisphere, that about 80% of fallout in the Gambier was due to fallout from the Moruroa and Fangataufa tests. We can assess the close-in tropospheric deposition in the Gambier relative to the stratospheric deposition from the signatures shown in Table 7 and no longer from the GF signatures in Table 5. These proportions are given in Table 8, calculated according to the different isotopic ratios with Eq. (1). The proportions obtained with the different ratios are consistent. Close-in tropospheric fallout is about 90% for all sites except for Ga7 where it is of the order of 70%. The proportion of LF for the different radionuclides measured in the Gambier is calculated from the activity ratios of LF (Table 5) and stratospheric fallout (Table 7), considering that the LF/GF ratio of ^{137}Cs is 200/300 as indicated in Section 4.3.3. The proportion is about 40% for ^{137}Cs , ^{241}Am and ^{241}Pu , 75% for ^{238}Pu and 90% for $^{239+240}\text{Pu}$.

Table 8

Proportion (%) of close-in tropospheric fallout in the Gambier calculated (Eq.1) from different isotopic ratios.

Site	$^{137}\text{Cs}/^{239+240}\text{Pu}$	$^{238}\text{Pu}/^{239+240}\text{Pu}$	$^{241}\text{Am}/^{239+240}\text{Pu}$	$(^{240}\text{Pu}/^{239}\text{Pu})_{\text{AR}}$	$(^{241}\text{Pu}/^{239}\text{Pu})_{\text{AR}}$
Ga1	88 ± 1	88 ± 12	81 ± 4	85 ± 2	84 ± 2
Ga2	92 ± 1	82 ± 17	83 ± 4	89 ± 2	85 ± 2
Ga3	85 ± 1	47 ± 54	72 ± 6	83 ± 3	75 ± 3
Ga5	90 ± 1	77 ± 22	77 ± 5	83 ± 3	79 ± 3
Ga6	92 ± 1	85 ± 14	86 ± 3	90 ± 2	88 ± 2
Ga7	74 ± 2	60 ± 42	58 ± 10	74 ± 5	62 ± 7
Average inventory	88 ± 1	76 ± 23	78 ± 5	84 ± 3	81 ± 2

5. Conclusions

The inventories of ^{137}Cs ($499 \pm 34 \text{ Bq.m}^{-2}$), ^{241}Am ($11.3 \pm 1.2 \text{ Bq.m}^{-2}$), ^{241}Pu ($33.7 \pm 3.4 \text{ Bq.m}^{-2}$), ^{238}Pu ($6.82 \pm 0.87 \text{ Bq.m}^{-2}$) and $^{239+240}\text{Pu}$ ($113.0 \pm 5.9 \text{ Bq.m}^{-2}$), sum of ^{239}Pu ($106 \pm 11 \text{ Bq.m}^{-2}$) and ^{240}Pu ($14.7 \pm 1.7 \text{ Bq.m}^{-2}$), supplemented by the measurement of $(^{240}\text{Pu}/^{239}\text{Pu})_{\text{AR}}$, (0.040 ± 0.004) from which the $(^{241}\text{Pu}/^{239}\text{Pu})_{\text{AR}}$ was deduced (2.03 ± 0.31) 10^{-4} were conducted for six sites on four islands in the Gambier Archipelago (24°S) located more than 400 km from the former French Pacific test sites in French Polynesia. These inventories are higher, and unequally for the different isotopes, than the GF in the Southern Hemisphere at this latitude, while plutonium atom ratios are lower. Based on the isotopic ratios determined in Gambier and the isotopic signatures from the test sites of Moruroa and Fangataufa as well as those from GF, derived from those of the Northern Hemisphere, we have shown using a two-member mixing model that:

- the isotopic signatures from Moruroa and Fangataufa (Table 5), estimated from samples taken at the sites in 1996 (IAEA, 1998), are also those of the LF in Gambier, excepting the $^{137}\text{Cs}/^{239+240}\text{Pu}$, deduced from the measurement of $^{90}\text{Sr}/^{239+240}\text{Pu}$, for both test sites and the $(^{240}\text{Pu}/^{239}\text{Pu})_{\text{AR}}$ and $(^{241}\text{Pu}/^{239}\text{Pu})_{\text{AR}}$ at Fangataufa.
- the signatures of stratospheric and close-in tropospheric fallout coming from French tests can be considered as identical since the GF-Gambier-LF mixing line of $(^{240}\text{Pu}/^{239}\text{Pu})_{\text{AR}} - (^{241}\text{Pu}/^{239}\text{Pu})_{\text{AR}}$ is practically confounded with the linear regression of a series of measurements carried out by the HASL on stratospheric dust collected during the years 1960-1970 (Hardy et al., 1973). The signatures in 2018 of stratospheric deposits in the Southern Hemisphere, resulting from the mixture of tests of both hemispheres, are estimated at 21.9 ± 0.1 for $^{137}\text{Cs}/^{239+240}\text{Pu}$, 0.11 ± 0.05 for $^{238}\text{Pu}/^{239+240}\text{Pu}$, 1.03 ± 0.12 for $^{241}\text{Pu}/^{239+240}\text{Pu}$, 0.35 ± 0.05 for $^{241}\text{Am}/^{239+240}\text{Pu}$, 0.157 ± 0.011 for $(^{240}\text{Pu}/^{239}\text{Pu})_{\text{AR}}$ and $(8.28 \pm 0.18)10^{-4}$ for $(^{241}\text{Pu}/^{239}\text{Pu})_{\text{AR}}$. These ratios are compatible with those measured at Hiva Oa, located more than 1,000 km north of the Moruroa and Fangataufa test sites (Bouisset et al., 2018) and with those measured on the Australian continent in regions not affected by English-test debris (Everett et al., 2008 ; Tims et al., 2013).
- the signatures of the LF in Gambier are evaluated at 2.0 ± 0.4 for $^{137}\text{Cs}/^{239+240}\text{Pu}$, 0.045 ± 0.008 for $^{238}\text{Pu}/^{239+240}\text{Pu}$, 0.031 ± 0.009 for $^{241}\text{Am}/^{239+240}\text{Pu}$, 0.092 ± 0.027 for $^{241}\text{Pu}/^{239+240}\text{Pu}$, 0.0176 ± 0.0049 for $(^{240}\text{Pu}/^{239}\text{Pu})_{\text{AR}}$ and $(0.55 \pm 0.23)10^{-4}$ for $(^{241}\text{Pu}/^{239}\text{Pu})_{\text{AR}}$.
- the proportions of close-in tropospheric fallout from French tests, derived from LF and from those of stratospheric fallout, are about 90% for six ? sites and 70% for one site.
- the proportions due to close-in deposition of different radionuclides are uneven. They have been estimated at 40% for ^{137}Cs , ^{241}Pu and ^{241}Am , 75% for ^{238}Pu and 90% for $^{239+240}\text{Pu}$.

REFERENCES

- Bennett B.G., 1978. Environmental Aspects of Americium. Report EML-348, pp. 202.
- Bouisset P., Calmet D., 1997. Hyper pure gamma-ray spectrometry applied to low-level environmental sample measurement. In: International Workshop on the Status of Measurement Techniques for the identification of Nuclear Signatures, Geel, Belgium. Esararda report EUR 17312, 73-81.
- Bouisset P., Nohl M., Bouville A., Leclerc G., 2018. Inventory and vertical distribution of ^{137}Cs , $^{239+240}\text{Pu}$ and ^{238}Pu in soil from Raivavae and Hiva Oa, two French Polynesian islands in the southern hemisphere. *J. Environ. Radioact.* 183, 82-93.
- Buesseler K.O., Charette M.A., Pike S.M., Henderson P.B., Kipp L.E., 2018. Lingering radioactivity at the Bikini and Enewetak Atolls. *Sci. Total Environ.* 621, 1185-1198.
- Bunzl K., Kracke W., Schimmack W., 1995. Migration of fallout $^{239+240}\text{Pu}$, ^{241}Am and ^{137}Cs in the various horizons of a forest soil under pine. *J. Environ. Radioact.* 28, N° 1, 17-34.
- Chamizo E., Garcia-Leon M., Peruchena J.I., Cereceda F., Vidal V., Pinilla E., Miro C., 2011. Presence of plutonium isotopes, ^{239}Pu and ^{240}Pu , in soils from Chile. *Nucl. Instr. and Meth. B* 269, 3163-3166.
- Charmasson S., Radakovitch O., Arnaud M., Bouisset P., Pruchon A-S., 1998. Long-core profiles of ^{137}Cs , ^{134}Cs , ^{60}Co and ^{210}Pb in sediment near the Rhône river (northwestern Mediterranean sea). *Estuaries* 21 n°3, 367-378.
- Chiappini R., Pointurier F., Millies-Lacroix J.C., Lepetit G., Hemet P., 1999. ^{240}Pu ^{239}Pu isotopic ratios and $^{239+240}\text{Pu}$ total measurements in surface and deep waters around Mururoa and Fangataufa atolls compared with Rangiroa atoll (French Polynesia). *Sci. Total Environ.* 237/238, 269-276.
- Chiappini R., Taillade J.M., Brébion S., 1996. Development of a High-sensitivity Inductively Coupled Plasma Mass Spectrometer for Actinide Measurement in the Femtogram Range. *Journal of Analytical Atomic Spectrometry*, Vol.11, 497-503.
- Danesi P.R., Moreno J., Makarewicz M., Radecki Z., 2002. Residual radioactivity in the terrestrial environment of the Mururoa and Fangataufa Atolls nuclear Weapon test sites. *J. Radioanal. Nucl. Chem.*, Vol. 253, No. 1, 53-65.
- Drozdovitch V., de Vathaire F., Bouville A., 2020. Ground deposition of radionuclides in French Polynesia resulting from atmospheric nuclear weapons tests at Mururoa and Fangataufa atolls. *J. Environ. Radioact.* 214-215, 106176.
- Duffa C., Renaud P., Calmet D., 2001. Activités de ^{238}Pu et de $^{239+240}\text{Pu}$ dans les sols cultivés de la basse vallée du Rhône. *C. R. Acad. Sci. Paris, Earth Plan. Sci.* 333, 275-281.
- Dong W., Tims S.G., Fifield L.K., Guo Q., 2010. Concentration and Characterization of plutonium in soils of Hubei in central China. *J. Environ. Radioact.* 101, 29-32.
- DSCEN, 2013. Surveillance des atolls de Mururoa et de Fangataufa. Tome 1: Surveillance radiologique Année 2011 (synthèse). N° 85 DEF/DGA/DO/UM NBC/SCEN. pp. 63.
- Eriksson M., Lindhal P., Roos P., Dahlggaard H., Holm E., 2008. U, Pu, and Am signatures of the Thule hydrogen bomb debris. *Environ. Sc. Technol.* 42, 4717-4722.
- Everett S.E., Tims S.G., Hancock G.J., Bartley R., Fifield L.K., 2008. Comparison of Pu and ^{137}Cs as tracers of soil and sediment transport in a terrestrial environment. *J. Environ. Radioact.* 99, 383-393.
- Froehlich M.B., Akber A., McNeil S.D., Tims S.G., Fifield L.K., Wallner A., 2019. Anthropogenic ^{236}U and Pu at remote sites of the South Pacific. *J. Environ. Radioact.* 205-206, 17-23.
- Gauthier-Lafaye F., Pourcelot L., Eikenberg J., Beer H., Le Roux G., Rhikvanov L. P., Stille P., Renauc Ph., Mezhibir A., 2008. Radioisotope contaminations from releases of the Tomsk-Seversk nuclear facility (Siberia, Russia). *J. Environ. Radioact.* 99, 680-693.
- Handl J., Sachse R., Jakob D., Michel R., Evangelista H., Gonçalves A.C., de Freitas A.C., 2008. Accumulation of ^{137}Cs in Brazilian soils and its transfer to plants under different climatic conditions. *J. Environ. Radioact.* 99, 271-287.
- Hardy E.P., Krey P.W., Volchok H.L., 1972. Global inventory and distribution of Pu-238 from SNAP-9A. USAEC Report HASL-250, pp. 32.
- Hardy E.P., Krey P.W., Volchok H.L., 1973. Global Inventory and Distribution of Fallout Plutonium. *Nature* 241, 444-445.
- Hardy E.P., 1973. Fallout program. Quaterly summary report. Report HASL-273, pp. 229.
- Holm E., Riaseco J., Pettersson H., 1992. Fallout of transuranium elements following the Chernobyl accident. *J. Radioanal. Nucl. Chem.*, Vol. 156, No.1, 183-200

- Hrnecek E., Steier P., Wallner A., 2005. Determination of plutonium in environmental samples by AMS and alpha spectrometry. *Applied Radiation and Isotopes* 63, 633-638.
- Huang Y., Tims S.G., Froehlich M. B., Pan S., Fifield L.K., Pavetich S., Koll D., 2019. The $^{240}\text{Pu}/^{239}\text{Pu}$ atom ratio in Chinese soils. *Sci. Total Environ.* 678, 603-610.
- IAEA, 1998. The radiological situation at the atolls of Mururoa and Fangataufa. Technical report. Volume 1: Radionuclide concentrations measured in the terrestrial environment of the atolls. Report by an international advisory committee. pp. 278.
- Irlweck K., Hrnecek E., 1999. ^{241}Am concentration and $^{241}\text{Pu}/^{239(240)}\text{Pu}$ ratios in soils contaminated by weapons-grade plutonium. *J. Radioanal. Nucl. Chem.*, Vol. 242, No.3, 595-599.
- Johansen M.P., Child D.P., Davis E., Doering C., Harrison J.J., Hotchkis M.A.C., Payne T.E., Thiruvoth S., Twining J.R., Wood M.D., 2014. Plutonium in wildlife and soils at the Maralinga legacy site: persistence over decadal time scales. *J. Environ. Radioact.* 131, 72-80.
- Kelley J.M., Bond L.A., Beasley T.M., 1999. Global distribution of Pu isotopes and ^{237}Np . *Sci. Total Environ.* 237/238, 483-500.
- Kinoshita N., Sumi T., Takimoto K., Nagaoka M., Yokoyama A., Nakanishi T., 2011. Anthropogenic Pu distribution in Tropical East Pacific. *Sci. Total Environ.* 409, 1889-1999.
- Koide M., Michel R., Goldberg E., 1979. Depositional history of artificial radionuclides in the Ross Ice Shelf, Antarctica. *Earth Planet. Sci. Lett.* 44, 205-223.
- Koide M., Goldberg E.D., Hodge V.F., 1980. ^{241}Pu and ^{241}Am in sediments from coastal basins off California and Mexico. *Earth Planet. Sci. Lett.* 48, 250-256.
- Komosa A., 1999. Migration of plutonium isotopes in forest soil profiles in Lublin region (Eastern Poland). *J. Radioanal. Nucl. Chem.*, Vol.240, No.1, 19-24.
- Krey P.W., 1967. Atmospheric Burnup of a Plutonium-238 Generator. *American Association for the Advancement of Science, New Series*, Vol. 158, No. 3802, 769-771.
- Krey P.W. and Krajewski B., 1970. Comparison of atmospheric transport model calculations with observations of radioactive debris. *J. Geophys. Res.* 75, n° 15, 2901-2908.
- Krey P.W., Hardy E.P., Pachucki C., Rourke F., Coluzza J., Benson W.K., 1976. Mass isotopic composition of global fall-out plutonium in soil. *IAEA-SM-199/39*, 671-678.
- Le Roux G., Duffa C., Vray F., Renaud P., 2010. Deposition of artificial radionuclides from atmospheric Nuclear Weapon Tests estimated by soil inventories in French areas low-impacted by Chernobyl. *J. Environ. Radiact.* 101, 211-218.
- Lindhal P., Lee S-H., Worsfold P., Keith-Roach M., 2010. Plutonium isotopes as tracers for ocean processes: A review. *Mar. Environ. Res.* 69, 73-84.
- Lindhal P., Asami R., Iryu Y., Worsfold P., Keith-Roach M., Choi M-S., 2011. Sources of plutonium to the tropical Northwest Pacific Ocean (1943-1999) identified using a natural coral archive. *Geochim. Cosmochim. Acta* 75, 1346-1356.
- Livingston H.D., Schneider D.L., Bowen V.T., 1975. ^{241}Pu in the marine environment by a radiochemical procedure. *Earth Planet. Sci. Lett.* 25, 361-367.
- MINDEF, 2006. La dimension radiologique des essais nucléaires français en Polynésie - A l'épreuve des faits. pp. 474.
- Mitchell P.I., Sanchez-Cabeza J.A., Ryan T.P., McGarry A.T., Vidal-Quatras A., 1990. Preliminary estimates of cumulative caesium and plutonium deposition in the Irish terrestrial environment. *J. Radioanal. Nucl. Chem.* 138, N° 2, 241-256.
- Mitchell P.I., Leon Vintro L., Dahlgard H., Gasco C., Sanchez-Cabeza J.A., 1997. Perturbation in the $^{240}\text{Pu}/^{239}\text{Pu}$ global fallout ratio in local sediments following the nuclear accidents at Thule (Greenland) and Polomares (Spain). *Sci. Total Environ.* 202, 147-153.
- Muramatsu Y., Hamilton T., Uchida S., Tagami K., Yoshida S., Robison W., 2001. Measurement of $^{240}\text{Pu}/^{239}\text{Pu}$ isotopic ratios in soils from the Marshall Islands using ICP-MS. *Sci. Total Environ.* 278, 151-159.
- Orzel J., Komosa A., 2014. Study on the rate of plutonium vertical migration in various soil types of Lublin region (Eastern Poland). *J. Radioanal. Nucl. Chem.* 299, 643-649.
- Pourcelot L., Louvat D., Gauthier-Lafaye F., Stille P., 2003. Formation of radioactivity enriched soils in mountain areas. *J. Environ. Radiact.* 68, 215-233.
- Popof L., Mihailova G., Naidenov L., 2010. Determination of activity ratios of $^{238,239+240}\text{Pu}$, ^{241}Am , $^{134,137}\text{Cs}$, and ^{90}Sr in Bulgarian soils. *J. Radioanal. Nucl. Chem.* 285, 223-237.

- Rääf C., Holm E., Rabesiranana N., Garcia-Tenorio R., Chamizo E., 2017. On the presence of plutonium in Madagascar following the SNAP-9A satellite failure. *J. Environ. Radiact.* 177, 91-99.
- Schuller P., Voigt G., Handl J., Ellies A., Oliva L., 2002. Global weapons' fallout ^{137}Cs in soils and transfer to vegetation in south-central Chile. *J. Environ. Radiact.* 62, 181-193.
- Smith B.S., Child D.P., Fierro D., Harrison J.J., Heijnis H., Hotchkis M.A.C., Johansen M.P., Marx S., Payne T.E., Zawadzki A., 2016. Measurement of fallout radionuclides, $^{239,240}\text{Pu}$ and ^{137}Cs , in soil and creek sediment: Sydney Basin, Australia. *J. Environ. Radioact.* 151, 579-586.
- Thakur P., Khaing H., Salminen-Paatero S., 2017. Plutonium in the atmosphere: A global perspective. *J. Environ. Radioact.* 175-176, 39-51.
- Tims S.G., Keith Fifield L., Hancock G.J., Lal R.R., Hoo W.T., 2013. Plutonium isotope measurements from across continental Australia. *Nucl. Instr. and Meth. in Physics Research B* 294, 636-641.
- Tims S.G., Froehlich M.B., Fifield L.K., Walner A., De Cesare M., 2016. ^{236}U and $^{239,240}\text{Pu}$ ratios from soils around an Australian nuclear weapons test site. *J. Environ. Radioact.* 151, 563-567.
- Turner M., Rudin M., Cizdziel J., Hodge V., 2003. Excess plutonium in soil near the Nevada Test Site, USA. *Environmental Pollution* 125, 193-203.
- Ueda S., Ohtsuka Y., Kondo K., 2004. Inventories of $^{239+240}\text{Pu}$, ^{137}Cs , and excess ^{210}Pb in sediment cores from brackish Lake Obuchū, Rokkasho Village, Japan. *J. Radioanal. Nucl. Chem.* 261, N°2, 277-282.
- UNSCEAR, 2000. Sources and Effects of Ionizing Radiation. Volume I: Sources. Annex C: Exposures to the public from man-made sources of radiation. United Nations, New York. 158-291.
- Varga Z., 2007. Origin and release date assessment of environmental plutonium by isotopic composition. *Anal. Bioanal. Chem.* 389, 725-732.
- Warneke T., Croudace I. W., Warwick P.E., Taylor R.N., 2002. A new ground-level fallout record of uranium and plutonium isotopes for northern latitudes. *Earth Planet. Sci. Lett.* 203, 1047-1057.